A Variational Approach to Planning, Allocation and Mapping in Robot Swarms using Infinite Dimensional Models

by

Karthik Elamvazhuthi

A Thesis Presented in Partial Fulfillment
of the Requirement for the Degree
Master of Science

Approved November 2014 by the
Graduate Supervisory Committee:

Spring Berman, Chair
Matthew Peet
Hans Mittelmann

ARIZONA STATE UNIVERSITY

December 2014

ABSTRACT

This thesis considers two problems in the control of robotic swarms. Firstly, it addresses a trajectory planning and task allocation problem for a swarm of resource-constrained robots that cannot localize or communicate with each other and that exhibit stochasticity in their motion and task switching policies. We model the population dynamics of the robotic swarm as a set of advection-diffusion- reaction (ADR) partial differential equations (PDEs). Specifically, we consider a linear parabolic PDE model that is bilinear in the robots' velocity and task-switching rates. These parameters constitute a set of time-dependent control variables that can be optimized and transmitted to the robots prior to their deployment or broadcasted in real time. The planning and allocation problem can then be formulated as a PDE-constrained optimization problem, which we solve using techniques from optimal control. Simulations of a commercial pollination scenario validate the ability of our control approach to drive a robotic swarm to achieve predefined spatial distributions of activity over a closed domain, which may contain obstacles. Secondly, we consider a mapping problem wherein a robotic swarm is deployed over a closed domain and it is necessary to reconstruct the unknown spatial distribution of a feature of interest. The ADR-based primitives result in a coefficient identification problem for the corresponding system of PDEs. To deal with the inherent ill-posedness of the problem, we frame it as an optimization problem. We validate our approach through simulations and show that reconstruction of the spatially-dependent coefficient can be achieved with considerable accuracy using temporal information alone.

To Appa and Amma

ACKNOWLEDGEMENTS

Firstly, I would like to thank my advisor, Dr. Spring Berman for her unflinching support and great amount of patience shown throughout the course of this graduate program. Secondly, I would like to thank Dr. Matthew Peet, whose class on Modern Optimal Control motivated much of the mathematical discipline that I have tried to maintain through the course of this thesis. I would also like to thank Dr. Hans Mittelmann for all the knowledge on Optimization that helped me prepare for my work. Special thanks to Dr. Hendrik Kuiper for our multiple discussions on theory of Partial Differential Equations which made much of this thesis possible, and to Dr. Matthias Kawski for his insights on Optimal Control theory.

I would also like to thank my lab members and friends: Sean Wilson, Ted Pavlic, Ganesh Kumar, Ruben Gameros, Chase Adams, Ragesh Ramachandran, Shiba Biswal, Reza Kamyar, Monica Vuppalapati and Saketh Parnajape. They made this journey enjoyable. Most importantly I would like to thank my parents and brother for all their love and support.

TABLE OF CONTENTS

CHAPTER Page

Chapter 1

INTRODUCTION

In recent years there has been considerable interest in the use of robotic systems to augment or supersede human capabilities in performing complex tasks. This has been primarily due to the explosion in the number of opportunities resulting from advances in computing, communication, electronics, materials and mechanics. One class of interesting problems is that of multi-robot systems. Muti-robot systems are useful in scenarios where it might not be possible to perform the tasks required by a single robot alone. This might be either due to the number of tasks and the concurrent time constraints involved, or to exploit the redundancy offered by multiple robots. This redundancy might be especially motivated by the economical, actuation and environmental constraints in various real world applications that limit the complexity of a single robot. Typical examples of applications include mapping, surveillance, reconnaissance, and collective motion.

While a considerable amount of work has been done on trajectory planning, task allocation and mapping problems for the single robot case, the spatially distributed nature of multi-robot systems introduces several additional complexities. One of the main problems in extending work on single robots to muliple ones is that of scalability of the design methodologies. Scaling can be an issue in multiple aspects of system operation, such as computation, control and communication. Extension of single robot methods often results in explosion of the joint state space and has an adverse effect on computational tractability. This is more of a problem in the swarm paradigm of multi-robot systems, where the number of agents can go from hundreds to thousands and even in the trillions in the case of bio-medical applications. Managing this problem either involves some modeling assumptions or imposing certain physical or communication constraints on the system, so that the

resulting problem becomes tractable and the system behavior predictable. Managing the trade off between imposing such constraints and reduction in the range of target behaviors is often a challenge. Many times these constraints might even be naturally imposed on the system and physically unavoidable. This is especially the case in nano-robotic applications where agents work under severe actuation and sensory limitations.

The swarm paradigm considered in this work can be partly motivated by several natural phenomena. It is often the case that simple animal behaviors, when performed in parallel by large populations, show quite complex global behaviors. Where as it has been the goal mathematical biology to predict these natural phenomena and understand the basic primitives that agents in these systems follow, in robotics the application is subtly different in that, it is usually the goal to understand the suitable primitives that should be assigned to the each of the agents so that the resulting behavior can be abstracted suitably. This should result in computationally tractable models that are amenable to analysis and can aid in design decisions so that desired target behaviors can be guaranteed.

1.1 Literature Review

This section mentions some relevant work in the field of swarm robotics using advection diffusion models and optimal control of bilinear and multiplicative control systems of partial differential equations.

Many instances of PDE based modeling can be found in mathematical biology literature. Flocking [Ha and Tadmor (2008)], schooling [Okubo (1986)] and other such herd behavior are modeled often using PDEs [Murray (2002)]. This is usually some type of nonlinear diffusion equation, wherein each agent changes its state based on the local observations and interaction. Another application in modeling of biological systems is that of chemotaxis [Stevens and Othmer (1997)] and foraging behavior in swarms. Similar models can also be found in modeling spatio-temporal evolution of bee colonies and their pollina-

tion behavior [Sánchez-Garduño and Breña-Medina (2011)]. The underlying microscopic interactions of the agents usually have a corresponding stochastic model. This is similar to modeling of Brownian agents where the evolution probability densities of these agents can be described using Fokker-Planck equations [Gardiner (1985)].

On these same principles chemical reation networks have been used to model robots that show probabilistic decision making [Matthey *et al.* (2009)]. Fokker-Planck equations have been used to model spatial inhomogeniety of swarms that show similar probabilistic decision and motion primitives, however without the well mixed assumption that is typical of CRN models. [Hamann and Worn (2007)] considers modeling such swarms with local interaction between robots and hence predictability of macroscopic description from such local interactions. Similar work has been done in [Galstyan *et al.* (2005)] for a nanorobotics application where robots in a biological medium respond to changes in density of a chemical. [Prorok *et al.* (2011)] studied the use of Fokker- Planck equations for analysis of spatial effects of robots with stochastic state transitions. The issue of optimization of robot behavior has received some attention in this framework. In this direction [Milutinovic and Lima (2006)] has done some work on optimizing state transition of robots with drift to maximize their distribution over some desired region. They extended their work to optimizing stochastic robot behavior modeled by a nonlinear Fokker-Planck equation [Palmer and Milutinovic (2011)]. Such work can be compared to that of [Foderaro (2013)], that also considered spatially dependent velocity fields for a formation control problem.

Control systems that have a similar structure can also be found in many other applications in literature. These typically fall under the banner of bilinear [Elliott (2009)] or multiplicative control systems (MCS) [Khapalov (2010)]. The previously mentioned systems fall under this class of control systems. MCS are systems where the controls multiply with the states through a (linear or non-linear) operator acting on the states. A bilinear control system corresponds to a MCS that is linear in the initial conditions for fixed controls.

[Finotti *et al.* (2012)] and [Lenhart (1995)] use optimal control to study the effect of resource distribution over an environment on the movement of a population. [Belmiloudi (2008)] consider a min-max problem for diffusion type models, where the reactions are the main controls. They show the effectiveness of their method on a nuclear reactor model. Other works on optimal control of bilinear PDEs include [Boulerhcha *et al.* (2012)] [Tagiev (2009)] [Casas and Wachsmuth (2014)]. Aside from optimal control, some studies have also been conducted on the controllability properties of such systems [Ball *et al.* (1982)] [Khapalov (2010)] [Beauchard and Coron (2006)]. This has also been applied in a robotic setting where controllability properties are considered under a uniform control input for a swarm of robots with inhomogenous turning rates [Becker *et al.* (2012)]. [Kachroo (2009)] considers the control and stabilization of vehicle traffic systems that are modeled by advection type systems. The optimal control methodology used in this work can be found in [Tröltzsch (2010)] [Pinnau and Ulbrich (2008)] [Belmiloudi (2008)].

There has been very little work on the problem of simultaneous trajectory planning and task allocation. An example is the work presented in [Turpin *et al.* (2014)]. The problem considered in this work involves a number of point agents with first order dynamics whose trajectories need to be computed and tasks are needed to be assigned to robots without any preference, i.e. there is no preference as to which robot is assigned which task.

1.2 Contribution

This thesis presents a control theoretic approach to the problem of optimization of combined path planning and allocation of swarm of robots modeled using advection-diffusion-reaction (ADR) partial differential equations (PDEs) equations. More specifically, it considers the optimal control approach. Optimal control is the generalization of optimization in finite dimensional spaces to minimization (or maximization) of objective functionals that are constrained by system of ordinary or partial differential equation (or other evolu-

tion systems). Optimal control results in a computationally efficient method to compute the controls as compared to black box approaches to optimization. Black box approaches such as stochastic optimization, genetic algorithms and particle swarm optimization methods are computationally too inefficient for the purpose of controller synthesis due to number of evaluations of objective functional required in the optimization cycles. Optimal control methods in contrast take advantage of the structure of the problem by characterizing the gradient using the adjoint equation. This reduces the complexity of computing the gradient of the objective functional. We frame the planning and allocation problem as an optimal control problem. Subsequently we present some theoretical analysis characterizing the optimal controls. This is in turn is used to realize an algorithm to numerically approximate the optimal controls. A part of this section subsection 4.1.1 subsection 4.1.3 subsection 4.1.4 has been submitted to a peer-reviewed conference [Elamvazhuthi and Berman (2015)].

Additionally, we consider the problem of mapping regions of interest in an unknown environment using encounter-based observations from robotic swarms. We show that even with noise-induced agent behaviors of the agents, a rich map of the environment can be constructed with temporal information extracted from the robots. We pose the resulting system as optimization problem, which is solved numerically using a gradient descent method as for the optimal control problem.

1.3 Problem Statement

The first scenario under consideration involves swarm of robotic bees that must pollinate several rows of crops. The model of the robots are motivated by recent work on flapping wing micro aerial vehicles such as the Robobee [Ma *et al.* (2013)]. As in the work of [Berman *et al.* (2011b)], we aim to design robot control policies that produce a uniform density of flower visits along crop rows, and that can achieve any ratio between numbers of flower visits at plants in different rows. In contrast to the work in [Berman *et al.* (2011b)],

we consider environments that are bounded rather than unbounded and that may contain obstacles. Additionally, the optimization methodolgy is based on optimal control theory rather than stochastic optimization methods.

The second scenario involves a smaller swarm of agents that are deployed in order to map an environment of interest. We regularize the the inverse problem using the well known Tikhonov regularization. The optimization approach helps construct a simple yet efficient convergent algorithm that is able to reconstruct the map of a feature of interest in the environment, which could be the distribution of crops in the pollination scenario.

1.3.1 Robot Capabilities

The robots would have sufficient power to undertake brief flights that originate from a location called the *hive*, and they would return to the hive to recharge. A computer at the hive can serve as the supervisory agent in our architecture. The computer calculates the parameters of the robot motion and task transitions for a specified pollination objective and transmits these parameters to the robots when they are docked at the hive for charging and uploading data. During a flight, the robots are assumed to be capable of recognizing a flower that is very close by, distinguishing between different types of flowers, flying to a flower, and hovering briefly while obtaining pollen from the flower using an appropriate appendage. Each robot is equipped with a compass and thus can fly with a specified heading. We also assume that robots can detect obstacles within their local sensing range and adjust their flight path to avoid collision. Notably, the robots are not assumed to have localization capabilities, since it is infeasible to use GPS sensors on highly power-constrained platforms.

1.3.2 Robot Controller

Each member of a swarm of N robots performs the following actions during a flight. Upon deploying from the hive, each robot flies with a time-dependent velocity $\mathbf{v}(t) \in \mathbb{R}^2$. Concurrently with this deterministic motion, the robot exhibits random movement that arises from inherent noise due to sensor and actuator errors. We assume that the flowers are distributed densely enough such that a robot can always detect at least one flower in its sensing range when it flies over plants. While a robot is flying over a row with flowers of type j, it decides with a time-dependent probability per unit time, $k_j(t)$, to pause at a flower in its sensing range and hover for pollination. The robot resumes flying with a fixed probability per unit time k_f, which determines the time taken to pollinate. The optimal control approach described in section 4.1 computes the parameters $\mathbf{v}(t)$ and $k_j(t)$ prior to the robots' flight.

Chapter 2

MODELS OF THE COVERAGE SCENARIOS

In this chapter we describe the microscopic and macroscopic models for the swarm of agents. The microscopic model is a stochastic agent based model based on theory of stochastic differential equations [Gardiner (1985)]. It accounts for stochasticity in the agents' state evolution and is used to validate the control and estimation approaches described in the sequel. The macroscopic models are deterministic models defined using a systems of PDEs. The macroscopic models define the mean population dynamics of the microscopic models.

2.1 Planning and Allocation

2.1.1 Microscopic Model

The microscopic model is used to simulate the individual robots' motion and probabilistic decisions that are produced by the robot controller in subsection 1.3.2. We model a robot's changes in state as a Chemical Reaction Network (CRN) in which the species are F, a flying robot; H_j, a robot that is hovering over a flower of type j; and V_j, an instance of a robot visit to a flower of type j. The reactions are:

$$F \xrightarrow{k_j(t)} H_j + V_j \tag{2.1}$$

$$H_j \xrightarrow{k_f} F \tag{2.2}$$

A robot i has position $\mathbf{x}_i(t) = [x_i(t)\ y_i(t)]^T$ at time t. The deterministic motion of each flying robot is governed by the time-dependent velocity field $\mathbf{v}(t) = [v_x(t)\ v_y(t)]^T$. The robot's random movement is modeled as a Brownian motion that drives diffusion with an

associated diffusion coefficient D, which we assume that we can characterize. We model the displacement of the robot over each timestep Δt using the standard-form Langevin equation [Gillespie (2000)],

$$\mathbf{x}_i(t+\Delta t) - \mathbf{x}_i(t) = \mathbf{v}(t)\Delta t + (2D\Delta t)^{1/2}\,\mathbf{Z}(t), \tag{2.3}$$

where $\mathbf{Z} \in \mathbb{R}^2$ is a vector of independent, normally distributed random variables with zero mean and unit variance. When a robot encounters an obstacle or a wall, it avoids a collision by flying according to a specular reflection from the boundary.

2.1.2 Macroscopic Model

We can describe the time evolution of the expected spatial distribution of the swarm with a *macroscopic model* consisting of a set of advection-diffusion-reaction (ADR) partial differential equations [Berman *et al.* (2011a)]. The states of this model are the population density fields $y_1(\mathbf{x},t)$ of flying robots, $y_2(\mathbf{x},t)$ of hovering robots, and $y_3(\mathbf{x},t)$ of flower visit events. The velocity field $\mathbf{v}(t)$ and transition rates $k_j(t)$ are time-dependent control parameters. The model is defined over a bounded domain, $\Omega \subset \mathbb{R}^2$, with Lipschitz continuous boundary $\partial\Omega$. We define $Q = \Omega \times (0,T)$ and $\Sigma = \partial\Omega \times (0,T)$ for some fixed final time T. The vector $\mathbf{n} \in \mathbb{R}^2$ is the outward normal to $\partial\Omega$. There are n_f types of flowers, and the function $H_i : \Omega \to \{0,1\}$ is a spatially-dependent coefficient that models the presence ($H_i(\mathbf{x}) = 1$) or absence ($H_i(\mathbf{x}) = 0$) of flowers of type i at point $\mathbf{x}$ in the domain.

Given these definitions, the macroscopic model of the pollination scenario is defined as:

$$\begin{aligned}
\frac{\partial y_1}{\partial t} &= \nabla \cdot (D\nabla y_1 - \mathbf{v}(t) y_1) - \sum_{i=1}^{n_f} k_i H_i y_1 + k_f y_2 \;\; in \;\; Q, \\
\frac{\partial y_2}{\partial t} &= \sum_{i=1}^{n_f} k_i H_i y_1 - k_f y_2 \;\; in \;\; Q, \\
\frac{\partial y_3}{\partial t} &= \sum_{i=1}^{n_f} k_i H_i y_1 \;\; in \;\; Q,
\end{aligned} \tag{2.4}$$

with the no-flux boundary conditions

$$\vec{\mathbf{n}} \cdot (D\nabla y_1 - \vec{\mathbf{v}}(t) y_1) = 0 \ \ on \ \ \Sigma. \tag{2.5}$$

Initially, the flying robots are distributed according to a Gaussian density centered at a point $\mathbf{x}_0$, and there are no hovering robots or visits in the domain.

2.2 Mapping

2.2.1 Microscopic Model

The microscopic model for the mapping problem involves only one reaction. The reaction network is a modification of the one in Equation 2.1 and Equation 2.2. The main difference is that robots do not transition to hover state. When a flying robot F passes over a feature of interest there is probability per unit time k_0 that it registers an observation, O. The chemical reactions of this system is given by

$$F \ \xrightarrow{k_o} \ F + O \tag{2.6}$$

The robots will obey the motion model as in Equation 2.3. However, the velocity field, $\vec{v}$ is predefined so that the a trajectory is assigned to the agents, rather than optimized as in the previous case. The trajectory is chosen such that sufficient coverage of the domain can be ensured.

2.2.2 Macroscopic Model

A number of robots are assigned a predefined trajectory based on a time dependent velocity field. In the previous scenario knowledge of the spatial dependent coefficient, $H(x)$, is assumed. However, in the mapping scenario the spatial distribution of the feature of interest is unknown. It is required that agents register their observations as they pass

over these features over a domain. The resulting macroscopic model is of the form,

$$\begin{aligned}\frac{\partial y_1}{\partial t} &= \nabla \cdot (D\nabla y_1 - \mathbf{v}(t)y_1) \quad in\ \ Q,\\ \frac{\partial y_2}{\partial t} &= k_o H y_1,\end{aligned} \tag{2.7}$$

with the no-flux boundary conditions

$$\vec{\mathbf{n}} \cdot (D\nabla y_1 - \vec{\mathbf{v}}(t)y_1) = 0 \ \ on\ \ \Sigma. \tag{2.8}$$

It is required that the spatial coefficient, H, be reconstructed from information of the total number of observations. More specifically it is desired that the H is estimated using the total number of positive observations of the feature of interest at each time instant, i.e., no spatial information about the observation locations is required from the agents.

Chapter 3

MATHEMATICAL BACKGROUND

This chapter defines some mathematical terminologies that will be used in subsequent chapters. The information presented in this chapter has been adapted from [Tröltzsch (2010)] [Evans (1998)] [Pinnau and Ulbrich (2008)] and [Kurdila and Zabarankin (2006)].

3.1 Functional Analysis

Definition 3.1.1. *A normed space $\{X, \|\cdot\|\}$ is said to be complete if every cauchy sequence in X converges, i.e, has a limit in X. A complete normed space is called a Banach space.*

Definition 3.1.2. *A Hilbert Space H is a Banach space endowed with an inner product $(,)$ which generates the norm, i.e, $\|u\| = (u,u)^{1/2}$.*

Let X and Y be real Banach Spaces.

Definition 3.1.3. *A mapping $A : X \to Y$ is linear mapping or a linear operator if*

$$A(\lambda u + \mu u) = \lambda Au + \mu Au \tag{3.1}$$

for all $u, y \in X$ and $\lambda, \mu \in \mathbb{R}$.

Definition 3.1.4. *A linear operator $A : X \to Y$ is bounded if*

$$\|A\| := sup\{\|A\|_Y : \|u\|_X \leq 1\} < \infty. \tag{3.2}$$

Definition 3.1.5. *$\mathscr{L}(X,Y)$ denotes the normed space of all linear continuous mappings form X to Y, endowed with the norm $\|\cdot\|$. If $X = Y$, then we write $\mathscr{L}(X,Y) := \mathscr{L}(X)$.*

Definition 3.1.6. *The space $X^* := \mathscr{L}(X,\mathbb{R})$ of linear functionals on X is called dual space of X, with the associated norm*

$$\|f\|_{X^*} = \sup_{\|u\|_X=1} |f(u)|. \tag{3.3}$$

We use the notation

$$\langle f,u\rangle_{X^*,X} = f(u) \tag{3.4}$$

$\langle\cdot,\cdot\rangle_{X^*,X}$ is called the duality pairing of X^* and X.

Theorem 3.1.7. *(Reisz Representation theorem). Let $\{H,(\cdot,\cdot)_H\}$ be a real Hilbert space. Then for any linear functional $F \in H^*$ there exists a uniquely determined $f \in H$ such that $\|F\|_{H^*} = \|f\|_H$ and*

$$F(v) = (f,v)_H \ \ \forall v \in H. \tag{3.5}$$

Definition 3.1.8. *Let $1 \leq p < \infty$ and suppose Ω is a Lesbesgue measurable subset of $\mathbb{R}^n$. We define*

$$L^p(\Omega) = \left\{ f : \Omega \to \mathbb{R}, \|f\|_{L^p(\Omega)} = \left(\int_\Omega |f|^p \right)^{1/p} < \infty \right\} \tag{3.6}$$

while for $p = \infty$, we define

$$L^\infty(\Omega) = \left\{ f : \Omega \to \mathbb{R}, \|f\|_{L^\infty(\Omega)} = ess\sup_{x\in\Omega} |f(x)| < \infty \right\}. \tag{3.7}$$

Similarly,

$$L^p_{loc}(\Omega) = \left\{ f : \Omega \to \mathbb{R}, f \in L^p(K) \quad \forall K \subset \Omega \ \ Compact \right\} \tag{3.8}$$

.

Theorem 3.1.9. *(Fischer-Riesz) For $1 \leq p \leq \infty$, the spaces $L^p(\Omega)$ are Banach spaces. The space $L^2(\Omega)$ is a Hilbert Space with inner product*

$$(u,v)_{L^2(\Omega)} := \int_\Omega uv dx. \tag{3.9}$$

Definition 3.2.1. *Let $\Omega \subset \mathbb{R}^n$ be open and let $u \in L^1_{loc}(\Omega)$. If there exists a function $w \in L^1_{loc}$ such that*

$$\int_\Omega w\phi = (-1)^\alpha \int_\Omega u D^\alpha \phi dx, \quad \forall \phi \in C_0^\infty(\Omega) \tag{3.10}$$

then $D^\alpha u := w$ is called α-th weak partial derivative of u.

Definition 3.2.2. *Let $\Omega \subset \mathbb{R}^n$ be open. For $k \in \mathbb{N}_0$, $p \in [1,\infty)$, we define the Sobolev space, $W^{k,p}$ by*

$$W^{k,p} = \left\{ u \in L^p(\Omega) : D^\alpha u \quad \forall |\alpha| \leq k \right\} \tag{3.11}$$

endowed with the norm

$$\|u\|_{W^{k,p}(\Omega)} = \left(\sum_{|\alpha| \leq k} \int_\Omega |D^\alpha u(x)|^p dx \right)^{1/p}. \tag{3.12}$$

For $p = \infty$, $W^{k,\infty}(\Omega)$ is defined, equipped with the norm

$$\|u\|_{W^{k,\infty}} = \max_{|\alpha| \leq k} \|D^\alpha u\|_{L^\infty(\Omega)}. \tag{3.13}$$

For $p = 2$, we write $H^k(\Omega) := W^{k,2}(\Omega)$. We have

$$H^1(\Omega) = \left\{ u \in L^2(\Omega) : D_i u \in L^2(\Omega), i = 1, ..., N \right\} \tag{3.14}$$

and is endowed with the norm

$$\|u\|_{H^1(\Omega)} = \left(\int_\Omega (u^2 + |\nabla u|^2) \right)^{1/2} \tag{3.15}$$

with the inner product

$$(x,y)_{H^1(\Omega)} = \int_\Omega xy d\mu + \int_\Omega \nabla x \cdot \nabla y d\mu. \tag{3.16}$$

Theorem 3.2.3. *(Trace Theorem) Let $\Omega \subset \mathbb{R}^N$ be a bounded Lipschitz domain and let $1 \leq p \leq \infty$. Then there exists a linear and continuous mapping, $\tau : W^{1,p}(\Omega) \to L^p(\partial\Omega)$ such that for all $u \in W^{1,p}(\Omega) \cap C(\bar{\Omega}))$ we have $(\tau u)(x) = u(x)$ for all $x \in \Omega$.*

τ is called the trace operator. From linearity and continuity of the trace operator we can conclude there exists some constant $c = c(\Omega, p)$ such that

$$\|\tau u\|_{L^p(\Omega)} \leq c\|u\|_{W^{1,p}(\Omega)} \quad \forall u \in W^{1,p}(\Omega). \tag{3.17}$$

Let X be a separable Banach Space. We consider mappings $t \in [0,T] \to y(t) \in X$.

Definition 3.2.4. *1. A function $s : [0,T] \to X$ is called simple if it has the form*

$$s(t) = \sum_{i=1}^{m} 1_{E_i}(t) y_i, \tag{3.18}$$

with Lesbesgue measurable sets $E_i \subset [0,T]$ and $y_i \in X$

2. A function $f : t \in [0,T] \to f(t) \in X$ is called strongly measurable if there exist simple functions $s_k : [0,T] \to X$ such that

$$s_k(t) \to \quad f(t) \ \ for \ \ almost \ \ all \ \ t \in [0,T]. \tag{3.19}$$

Definition 3.2.5. *Let X be a separable Banach Space. We define for $1 \leq p < \infty$ the space*

$$L^p(0,T;X) := \Big\{ y : [0,T] \to X \ \ strongly \ \ measurable \ \ : \\ \|y\|_{L^p(0,T;X)} := \Big(\int_0^T \|y(t)\|_X^p dt \Big)^{1/p} < \infty \Big\}. \tag{3.20}$$

Moreover, we let

$$L^\infty(0,T;X) := \Big\{ y : [0,T] \to X \ \ strongly \ \ measurable \ \ : \\ \|y\|_{L^\infty(0,T;X)} := ess \sup_{t \in [0,T]} \|y(t)\|_X < \infty \Big\}. \tag{3.21}$$

The space $C^k([0,T];X)$, $k \in \mathbb{N}_0$ is defined as the space of k-times continuously differentiable functions on [0,T].

Definition 3.2.6. *(Weak time derivative) Let $y \in L^1(0,T;X)$. We say that $v \in L^1(0,T;X)$ is the weak derivative of y, written $y_t = v$, if*

$$\int_0^T \phi'(t)y(t) = -\int_0^T \phi(t)v(t)dt \quad \forall \phi \quad \in C_0^\infty(0,T). \tag{3.22}$$

Theorem 3.2.7. *Let X be a separable Banach space. Then for $1 \leq p < \infty$ the spaces $L^p(0,T;X)$ are Banach spaces. For $1 \leq p < \infty$ the dual space of $L^p(0,T;X)$ can isometrically be identified with $L^q(0,T;X^*)$, $\frac{1}{p} + \frac{1}{q} = 1$, by means of the pairing*

$$\langle v, y \rangle_{L^q(0,T);X*,L^p(0,T;X)} = \int_0^T \langle v(t), y(t) \rangle_{X^*,X} dt. \tag{3.23}$$

If H is a separable Hilbert space then $L^2(0,T;H)$ is a Hilbert space with inner product

$$(y,v)_{L^2(0,T;X)} := \int_0^T (y(t), v(t))_H dt. \tag{3.24}$$

Definition 3.2.8. *Let H, V be separable Hilbert spaces with continuous and dense embedding. We denote by $W(0,T;H,V)$ the linear space of all $y \in L^2(0,T;V)$ having a distributional time derivative $y' \in L^2(0,T;V^*)$, equipped with the norm*

$$\|y\|_{W(0,T;H,V)} = \left(\int_0^T \left(\|y\|_V^2 + \|y'(t)\|_{V^*}^2 \right) dt \right)^{1/2}. \tag{3.25}$$

Definition 3.2.9. *Let H, V be separable Hilbert spaces with continuous and dense embedding $V \hookrightarrow H$. We identify H with its dual H^*. Then we have the continuous and dense embeddings*

$$V \hookrightarrow H \cong H^* \hookrightarrow V^* \tag{3.26}$$

which is called the Gelfand Triple.

Theorem 3.2.10. *Let $V \hookrightarrow H \hookrightarrow V^*$ be a Gelfand Triple. Then we have the continuous embedding $W(0,T;H,V) \hookrightarrow C([0,T];H)$. Moreover, for all $y, p \in W(0,T;H,V)$ we have the integration by parts formula*

$$(y(T), p(T))_H - (y(0), p(0))_H = \int_0^T \langle y'(t), p(t) \rangle_{V^*,V} dt + \int_0^T \langle p'(t), y(t) \rangle_{V^*,V} dt. \tag{3.27}$$

Definition 3.3.1. *Let $F : U \subset X \to Y$ be an operator with U a non-empty subset. If the limit*

$$dF(u,h) := \lim_{t \downarrow 0} \frac{1}{t}(F(u+th) - F(u)) \tag{3.28}$$

exists in V, then it is called the direcitonal derivative of F at u in the direction h. If this limit exists for all $h \in U$, then the mapping $h \to dF(u,h)$ is termed the first variation of F at u.

Definition 3.3.2. *Suppose that the first variation $dF(u,h)$ at $u \in U$ exists, and suppose there exists a continuous linear operator $A : X \in Y$ such that*

$$dF(u,h) = Ah \ \ \forall h \in X. \tag{3.29}$$

Then F is said to be Gateaux differentiable at u, and A is referred to as the Gateaux derivative of F at u. We write A = F'(u).

Consider the problem

$$\min_{w \in W} J(w) \ \ s.t. \ \ w \in C \tag{3.30}$$

where W is a Banach space, $J : W \to \mathbb{R}$ is Gateaux differentiable and $C \subset W$ is non-empty closed and convex.

Theorem 3.3.3. *Let W be a Banach space and $C \subset W$ be nonempty and convex. Furthermore, let $J : W \to R$ be defined on an open neighborhood of C. Let w^* be a local solution of Equation 3.3 at which J is Gateaux-differentiable. Then the following optimality condition holds:*

$$\langle J'(w^*), w^* - w \rangle_{W*,W} \geq 0 \ \ \forall w \in C \tag{3.31}$$

Chapter 4

VARIATIONAL ANALYSIS

4.1 Planning and Allocation

In this section we consider the planning and allocation problem as an optimal control problem. Our algorithm for computing optimal control policies is based on the well-known gradient descent method. Methods of optimal control help to reduce the amount of computation that is required to compute the gradient of the objective functional with respect to the control, subject to constraints in the form of differential equations. This is done using the adjoint state equation. In the case of finite-dimensional systems, the adjoint/co-state equation can be derived using the Hamiltonian and Pontryagin's maximum principle. Efforts in optimal control of PDEs are in some sense attempts at generalization of the maximum principle. In the infinite-dimensional case the existence of the Hamiltonian has been proved only for a limited class of systems. For details of this approach refer to [Fattorini (1999)]. We study the solutions of PDEs in the 'weak' sense, as opposed to the 'mild' sense as in the semigroup theoretic setting in [Fattorini (1999)]. Further on we present some analysis regarding the existence of the optimal control, differentiability of the objective functional and a first order necessary condition.

First we define $V = H^1(\Omega)$ and $X = V \times L^2(\Omega)^n$. Consequently, we have $X^* := V^* \times L^2(\Omega)^n$ from Equation 3.2.9. We consider bilinear control systems in the following form for notational convenience:

$$\begin{aligned} &\frac{\partial y}{\partial t} = Ay + \sum_{i=1}^{m+2} u_i B_i y + f \ \ in \ \ Q,, \\ &\vec{n} \cdot (\nabla y_1 - \vec{u}_b y_1) = g \ \ in \ \ \Sigma \\ &y(0) = y_0. \end{aligned} \tag{4.1}$$

Q and Σ are as defined in subsection 2.1.2, the space time cylinder and the space time cylinder at the boundary respectively. Here, for $f \in F = L^2(0,T;L^2(\Omega)^{1+n})$, $g \in G = L^2(0,T;L^2(\partial\Omega)$ and $y_0 \in L^2(\Omega)^{1+n}$, we will understand a function, $y \in Y = L^2(0,T;X)$, $y_t \in Y^* = L^2(0,T;X^*)$, to be a weak solution of the the system, provided that:

$$\langle \frac{\partial y}{\partial t}, \phi \rangle_{Y^*,Y} = \langle A_g y, \phi \rangle_{Y^*,Y} + \sum_{i=1}^{m+2} \langle u_i B_i y, \phi \rangle_F + \langle f, \phi \rangle_F \tag{4.2}$$

for all $\phi \in L^2(0,T;X)$. For n =2, we have the following form for the operators A and $B_i : L^2(0,T;X) \to L^2(0,T;L^2(\Omega)^{1+n})$,

$$A = \begin{bmatrix} \nabla^2 & k_f & 0 \\ 0 & -k_f & 0 \\ 0 & 0 & 0 \end{bmatrix} \quad B_1 = \begin{bmatrix} -\frac{\partial}{\partial x_1} & 0 & 0 \\ 0 & 0 & 0 \\ 0 & 0 & 0 \end{bmatrix} \quad B_2 = \begin{bmatrix} -\frac{\partial}{\partial x_2} & 0 & 0 \\ 0 & 0 & 0 \\ 0 & 0 & 0 \end{bmatrix}$$
$$B_i = \begin{bmatrix} -H_{i-2} & 0 & 0 \\ H_{i-2} & 0 & 0 \\ H_{i-2} & 0 & 0 \end{bmatrix} \quad 3 \le i \le k_f + 2 \tag{4.3}$$

for all $\phi \in X$. $A_g : L^2(0,T;X) \to L^2(0,T;X^*)$ is the variational form of the operator A. The boundary conditions are equipped with A_g in the variational formulation using Green's theorem as,

$$A_g = \begin{bmatrix} M_g & k_f & 0 \\ 0 & -k_f & 0 \\ 0 & 0 & 0 \end{bmatrix} \tag{4.4}$$

Here, $M_g : L^2(0,T;V) \to L^2(0,T;V^*)$ is the Laplacian in the variational form and is defined as,

$$\left\langle M_g y, \phi \right\rangle_{V^*,V} = -\langle D\nabla y, \nabla\phi \rangle_{L^2(\Omega)} + \int_{\partial\Omega} (g + \vec{n} \cdot \vec{b} y)\phi dx \tag{4.5}$$

The solution of Equation 2.4 corresponds to A_0 and $f = 0$. We consider the more general

form for the purpose of analysis of differentiability properties of the control to state map (defined later) and the objective functional.

Also, the controls are $\vec{v} = (u_1, u_2) = \vec{u}_b$, $u_i = k_{i-2}$ for $3 \leq i \leq m+2$ and $m = n_f$.

Our optimal control problem can be framed as follows:

$$\min_{(y,u)\in Y\times U_{ad}} J(y,u) = \frac{1}{2}\|Wy(\cdot,T) - y_\Omega\|^2_{L^2(\Omega)^{1+n}} + \frac{\lambda}{2}\|u\|^2_{L^2(0,T)^m} \tag{4.6}$$

subject to Equation 4.1 for $f = 0$ and $g = 0$. Here, y_Ω is the target spatial distribution of robot activity, $Y = C([0,T], L^2(\Omega)^{1+n})$, and

$$U_{ad} = \{u \in L^2(0,T)^{m+2};\ u_i^{min} \leq u_i \leq u_i^{max}\ \ a.e.\ in\ \ (0,T)\}$$

is the set of admissible control inputs. Note that, due to the essential bounds on u, we have that $u \in L^\infty(0,T)^{m+2}$. Additionally, we take $W \in \mathscr{L}(L^2(\Omega)^{m+2})$. W is typically a weighting function that weights relative significance of minimizing the distance between different states and their targets.

4.1.1 Energy Estimates

Energy estimates refer to bounds on the solutions of the system under investigation with respect to some parameters of interest, such as initial condition, coefficients, boundary input. etc. While in theory of weak solutions of PDEs these energy estimates are used to show the existence of solutions, in the optimal control analysis, these are used to study the differentiability properties of the control to state map. We derive such energy estimates for the solutions of Equation 4.1.

Lemma 4.1.1. *Let $\vec{b} \in \mathbb{R}^2$ and $g \in L^2(\partial\Omega)$. Define $M : V \to V^*$ as*

$$\langle My, \phi\rangle_{V^*,V} = \langle D\nabla y, \nabla\phi\rangle_{L^2(\Omega)} - \int_{\partial\Omega}(g + \vec{n}\cdot\vec{b}y)\phi\, dx \tag{4.7}$$

for some $D > 0$. Then we have the following energy estimate for all $y \in V$

$$\beta\|y\|_V^2 \leq \langle My, y\rangle_{V^*,V} + \alpha(\|g\|^2_{L^2(\partial\Omega)} + \|y\|_H^2) \tag{4.8}$$

for some $\beta, \alpha > 0$.

Proof. Setting $\phi = y$ in the definition, we get,

$$D\int_\Omega |\nabla y|^2 dx \leq \langle My, y\rangle_{V^*,V} + \int_{\partial\Omega}(g + \vec{n}\cdot\vec{b}y)y dx \tag{4.9}$$

$$D\int_\Omega |\nabla y|^2 dx \leq \langle My, y\rangle_{V^*,V} + \int_{\partial\Omega}|g||y|dx + |b|\int_{\partial\Omega}|y|^2 dx \tag{4.10}$$

$$D\|y\|_V^2 \leq \langle My, y\rangle_{V^*,V} + \frac{1}{2}\|g\|^2_{L^2(\partial\Omega)} + \frac{1}{2}\|\tau y\|^2_{L^2(\partial\Omega)} + |b|\|\tau y\|^2_{L^2(\partial\Omega)} + D\|y\|_H^2 \tag{4.11}$$

Using the bounds on trace operator Equation 3.2, the result follows. □

That M is indeed a mapping from V to V^* can be verified using bilinear forms as in [Evans (1998)] and [Grubb (2008)].

Corollary 4.1.2. *Define $A_g : X \to X^*$ be as in Equation 4.1 then we have the following energy estimate*

$$\beta\|y\|_X^2 \leq -\langle Ay, y\rangle_{X^*,X} + \alpha(\|g\|^2_{L^2(\partial\Omega)} + \|y\|^2_{L^2(\Omega)^{1+n}}). \tag{4.12}$$

Lemma 4.1.3. *Consider the time dependent second order partial differential operators in their variational form, $L : L^2(0,T;V) \to L^2(0,T;V^*)$, $L^* : L^2(0,T;V) \to L^2(0,T;V^*)$ as,*

$$\begin{aligned}\langle Ly(t), \phi\rangle_{V^*,V} &= -\langle D\nabla y, \nabla\phi\rangle_{L^2(\Omega)} - \langle \vec{v}\cdot\nabla y, \phi\rangle_{L^2(\Omega)} + \int_{\partial\Omega}\vec{n}\cdot(\vec{v}y\phi)dx \\ \langle L^* p(t), \phi\rangle_{V^*,V} &= -\langle D\nabla p, \nabla\phi\rangle_{L^2(\Omega)} + \langle \vec{v}\cdot\nabla p, \phi\rangle_{L^2(\Omega)}.\end{aligned} \tag{4.13}$$

for all $\phi \in V$ then

$$\langle Ly, p\rangle_{V^*,V} - \langle y, L^* p\rangle_{V,V^*} = 0 \tag{4.14}$$

for all $y, p \in L^2(0,T;V)$. Moreover,

$$\left\langle L_g w(t), p\right\rangle_{V^*,V} - \langle w, L^* p(t)\rangle_{V,V^*} = g(t) \tag{4.15}$$

for all $w, p \in L^2(0,T;V)$ and

$$\langle L_g w(t), \phi\rangle_{V^*,V} = \langle Lw(t), \phi\rangle_{V^*,V} + \int_{\partial\Omega} g\phi dx \tag{4.16}$$

Proof. From Green's theorem [Evans (1998)] we have that,

$$\langle L^* p(t), \phi\rangle_{V^*,V} = -\langle D\nabla p, \nabla\phi\rangle_{L^2(\Omega)} - \langle \vec{v}\cdot p, \nabla\phi\rangle_{L^2(\Omega)} + \int_{\partial\Omega} \vec{n}\cdot(\vec{v}y\phi)dx. \tag{4.17}$$

□

Lemma 4.1.4. *Given $f \in L^2(0,T;L^2(\Omega))^{1+n}$, $g \in L^2(0,T;L^2(\partial\Omega))$ and the initial condition $y_0 \in L^2(\Omega)^{1+n}$, a unique solution exists for the problem in Equation 4.1. We have the following estimate for the unique solution y in $C([0,T];L^2(\Omega)^{1+n})$:*

$$\|y\|_{C([0,T];L^2(\Omega)^{1+n})} + \|y\|_{L^2(0,T;X)} \leq K(\|y_0\|_{L^2(\Omega)^{1+n}} + \|f\|_{L^2(0,T;L^2(\Omega))} + \|g\|_{L^2(0,T;L^2(\partial\Omega))} \tag{4.18}$$

where K depends only on Ω, $\max_{1\leq i\leq m+2}|u_i^{max}|$, $\max_{1\leq i\leq m+2}|u_i^{min}|$ and $\max_{1\leq i\leq m+2}|b_i|$.

Proof. Let $\phi = y$ in Equation 4.1. Then

$$\left\langle \frac{\partial y}{\partial t}, y\right\rangle_{X,X*} - \left\langle A_g y, y\right\rangle_{X,X*} = \sum_{i=1}^{p} \langle u_i B_i y, y\rangle_{L^2(\Omega)^{1+n}} + \langle f, y\rangle_{L^2(\Omega)^{n+1}} \tag{4.19}$$

. From Equation 4.1.2

$$\frac{d}{dt}\|y\|^2_{L^2(\Omega)^{1+n}} + \beta\|y\|^2_X \leq \sum_{i=1}^{p} \|u_i\|_{L^\infty(0,T)} \langle B_i y, y\rangle_{L^2(\Omega)^{1+n}} + \langle f, y\rangle_{L^2(\Omega)^{1+n}}$$
$$+\alpha(\|g\|^2_{L^2(\partial\Omega)} + \|y\|^2_H) \tag{4.20}$$

Using Cauchy's inequality and Young's inequality [Evans (1998)], we have

$$\frac{d}{dt}\|y\|^2_{L^2(\Omega)^{1+n}} + \beta\|y\|^2_X \leq \frac{1}{2}\sum_{i=1}^{p}\|u_i\|_{L^\infty(0,T)}(\|B_i y\|_{L^2(\Omega)^{1+n}}\|y\|_{L^2(\Omega)^{1+n}}) + \frac{1}{2}(\|f\|^2_{L^2(\Omega)^{1+n}} + \|y\|^2_{L^2(\Omega)^{1+n}}) + \alpha(\|g\|^2_{L^2(\partial\Omega)} + \|y\|^2_H) \tag{4.21}$$

Let $M = \max_{1\leq i\leq p}\left\{b_i p|u_i^{min}|, b_i p|u_i^{max}|\right\}$. Then,

$$\frac{d}{dt}\|y\|^2_{L^2(\Omega)^{1+n}} + \beta\|y\|^2_X \leq M(\|y\|_X\|y\|_{L^2(\Omega)^{1+n}}) + \frac{1}{2}(\|f\|^2_{L^2(\Omega)^{1+n}} + \|y\|^2_{L^2(\Omega)^{1+n}}) + \alpha(\|g\|^2_{L^2(\partial\Omega)} + \|y\|^2_{L^2(\Omega)^{1+n}}) \tag{4.22}$$

Using Young's inequality we get,

$$\frac{d}{dt}\|y\|^2_{L^2(\Omega)^{1+n}} + \beta\|y\|^2_X \leq \frac{\beta}{2}\|y\|^2_X + \frac{M^2}{2\beta}\|y\|^2_{L^2(\Omega)^{1+n}} + \frac{1}{2}(\|f\|^2_{L^2(\Omega)^{1+n}} + \|y\|^2_{L^2(\Omega)^{1+n}}) + \alpha(\|g\|^2_{L^2(\partial\Omega)} + \|y\|^2_{L^2(\Omega)^{1+n}}) \tag{4.23}$$

Hence,

$$\frac{d}{dt}\|y\|^2_{L^2(\Omega)^{1+n}} + \frac{\beta}{2}\|y\|^2_X \leq \frac{M^2}{2\beta}\|y\|^2_{L^2(\Omega)^{1+n}} + \frac{1}{2}(\|f\|^2_{L^2(\Omega)^{1+n}} + \|y\|^2_{L^2(\Omega)^{1+n}}) + \alpha(\|g\|^2_{L^2(\partial\Omega)} + \|y\|^2_{L^2(\Omega)^{1+n}}) \tag{4.24}$$

and

$$\frac{d}{dt}\|y\|^2_{L^2(\Omega)^{1+n}} + \frac{\beta}{2}\|y\|^2_X \leq C(\|y\|^2_{L^2(\Omega)^{1+n}} + \|f\|^2_{L^2(\Omega)^{1+n}} + \|g\|^2_{L^2(\partial\Omega)}) \tag{4.25}$$

Then we also have,

$$\frac{d}{dt}\|y\|^2_{L^2(\Omega)^{1+n}} \leq C(\|y\|^2_{L^2(\Omega)^{1+n}} + \|f\|^2_{L^2(\Omega)^{1+n}} + \|g\|^2_{L^2(\partial\Omega)}) \tag{4.26}$$

Setting $\eta(t) = C\|y(t)\|^2_{L^2(\Omega)^{1+n}}$ and $\psi(t) = C(\|f(t)\|^2_{L^2(\Omega)^{1+n}} + \|g(t)\|^2_{L^2(\partial\Omega)})$ and using Gromwall's lemma [Evans (1998)] we get,

$$\max_{0\leq t\leq T}\|y(t)\|^2_{L^2(\Omega)^{1+n}} \leq C(\|y_0\|^2_{L^2(\Omega)^{1+n}} + \|f\|^2_{L^2(0,T;L^2(\Omega)^{1+n})} + \|g\|^2_{L^2(\partial\Omega)}) \tag{4.27}$$

for all $t \in (0,T)$. Substituting this expression in Equation 4.1.1 and integrating in time, t, over $(0,T)$ we get

$$\|y\|^2_{L^2(0,T;X)} \leq C(\|y_0\|^2_{L^2(\Omega)^{1+n}} + \|f\|^2_{L^2(0,T;L^2(\Omega)^{1+n})} + \|g\|^2_{L^2(0,T);L^2(\partial\Omega)}) \tag{4.28}$$

From these estimates and using traditional Galerkin approximations as in [Evans (1998)], the existence and uniqueness of solutions follows for the problem Equation 4.1.

□

4.1.2 Existence of Optimal Control

In this section we study the existence of solution that for the formulated optimal control problem in section 4.1. We introduce the control-to-state mapping, Ξ: $U_{ad} \to Y$, that maps a control, u, to y, the corresponding solution defined through Equation 4.1 for $f = 0$ and $g = 0$. This will help us in studying the existence of the optimal control and the differentiability of the objective functional, J, further on.

Theorem 4.1.5. *An optimal control u^* exists that minimizes the objective functional $\hat{J}$.*

Proof. The functional $\hat{J}(u)$ is bounded from below. Therefore, the infimum can be achieved and $q = \inf_{u \in U_{ad}} \hat{J}(u)$ exists. Let $\{u^n\}_{n=1}^{\infty}$ be a minimizing sequence such that $\hat{J}(u_n) \to q$ as $n \to \infty$.

Now that the infimum can be attained we need to find an optimal pair (y^*, u^*), so that $J(y^*, u^*) = q$. U_{ad} is bounded and closed convex set and hence weak sequentially compact. Hence, there exists a subsequence $\{u^n\}_{n=1}^{\infty}$ such that,

$$u^n \rightharpoonup u^* \quad \text{in } L^2(0,T)^{m+2} \tag{4.29}$$

Similarly, we can extract a subsequence $y_n = \Xi(u_n)$ due to the uniform boundedness from Equation 4.1.4, such that,

$$y^n \rightharpoonup y^* \quad \text{in } L^2(0,T;X) \tag{4.30}$$

Further on, it is required to confirm that $\Xi(y^*) = u^*$, since we do not know if the Ξ is weakly continuous. From Aubin-Lions lemma [Simon (1986)] we have that,

$$y_1^n \to y_1^* \quad in \;\; L^2(0,T;L^2(\Omega)) \tag{4.31}$$

From the uniform boundedness of the following terms we can also conclude that,

$$\begin{aligned} \nabla y_1^n &\rightharpoonup \nabla y_1^* \quad in \;\; L^2(0,T;L^2(\Omega)) \\ \nabla y_1^n &\to \nabla y_1^* \quad in \;\; L^2(0,T;V^*) \\ \frac{\partial y^n}{\partial t} &\rightharpoonup \frac{\partial y^*}{\partial t} \quad in \;\; L^2(0,T;V^*) \\ k_f y_2^n &\rightharpoonup k_f y_2^* \quad in \;\; L^2(0,T;L^2(\Omega)) \end{aligned} \tag{4.32}$$

From strong convergence of y_1^n in $L^2(0,T;L^2(\Omega))$ and weak convergence of u^n in $L^2(0,T)^{m+2}$, we can further deduce that,

$$\begin{aligned} k_i^n H_i y_1^n &\rightharpoonup k_i H_i y_1^* \quad in \;\; L^2(0,T;L^2(\Omega)) \\ \vec{v}^n \nabla y_1^n &\rightharpoonup \vec{v} \nabla y_1^* \quad in \;\; L^2(0,T;V^*) \end{aligned} \tag{4.33}$$

Note that the first implication above is not generally true for product of two weakly converging sequences. To deal with the boundary terms we use Green's theorem to get,

$$\langle \vec{v}^n \cdot \nabla y_1^n, \phi \rangle_{L^2(0,T;L^2(\Omega))} + \int_0^T \int_{\partial\Omega} \vec{n} \cdot (\vec{v}^n y \phi) dx dt = -\langle \vec{v}^n \cdot y_1^n, \nabla \phi \rangle_{L^2(0,T;L^2(\Omega))} \tag{4.34}$$

for all $\phi \in L^2(0,T;V)$. Due to strong convergence of y_1^n in $L^2(0,T;L^2(\Omega))$ and weak convergence of $\vec{v}^n$ in $L^2(0,T)^2$,

$$\vec{v}^n \cdot y_1^n \rightharpoonup \vec{v}^* \cdot y_1^* \quad in \;\; L^2(0,T;L^2(\Omega)) \tag{4.35}$$

Due to the above mentioned convergences we have that the sequence of solutions $y^n = \Xi(u^n)$ given by,

$$\langle \frac{\partial y^n}{\partial t}, \phi \rangle_{Y^*,Y} = \langle A_0 y^n, \phi \rangle_{Y^*,Y} + \sum_{i=1}^{m+2} \langle u_i^n B_i y^n, \phi \rangle_F \tag{4.36}$$

converges to the solution $\Xi(u^*)$ and is given by,

$$\langle \frac{\partial y^*}{\partial t}, \phi \rangle_{Y^*,Y} = \langle A_0 y^*, \phi \rangle_{Y^*,Y} + \sum_{i=1}^{m+2} \langle u_i^* B_i y^*, \phi \rangle_F \tag{4.37}$$

It remains to be shown that $\hat{J}(u^*) = q$. J is weakly lower semicontinuous. Hence,

$$q = \lim_{n\to\infty} J(y^n, u^n) \leq J(y^*, u^*) \tag{4.38}$$

Since q is the infimum,

$$\hat{J}(u^*) = J(y^*, u^*) = q \tag{4.39}$$

□

4.1.3 Differentiability and the Reduced Problem

This section discusses the differentiability of the objective functional.

Proposition 4.1.6. *The mapping Ξ is Gateaux differentiable at every $u \in U_{ad}$, and its Gateaux derivative, $\Xi'(u) : U_{ad} \to Y$, evaluated at $h \in U_{ad}$, i.e. $\Xi'(u)h$, is given by the solution of the following equation:*

$$\begin{aligned} &\frac{\partial w}{\partial t} = Aw + \sum_{i=1}^{m+2} u_i B_i w + \sum_{i=1}^{m+2} h_i B_i y \\ &\vec{n} \cdot (\nabla w_1 - \vec{u_b} \cdot w_1) = \vec{n} \cdot (\vec{h_b} y_1) \\ &w(0) = 0. \end{aligned} \tag{4.40}$$

Proof. We define $y_\varepsilon = \Xi(u + \varepsilon h)$. We show that $y_\varepsilon \to y$ as $\varepsilon \to 0$. Define $g = y_\varepsilon - y$. Then we have,

$$\begin{aligned} &\frac{\partial g}{\partial t} = Ag + \sum_{i=1}^{m+2} (u_i + \varepsilon h) B_i g + \varepsilon \sum_{i=1}^{m+2} h_i B_i y \\ &\vec{n} \cdot (\nabla g_1 - (\vec{u_b} + \varepsilon \vec{h_b}) \cdot g_1) = \vec{n} \cdot (\varepsilon \vec{h_b} y_1) \\ &g(0) = 0. \end{aligned} \tag{4.41}$$

For ε sufficiently small, $u+\varepsilon h \in U_{ad}$. Thus, it follows from Theorem 1.1 that

$$\|g\|_{C([0,T];L^2(\Omega)^{1+n})} \leq C(\|\varepsilon \sum_{i=1}^{m+2} h_i B_i y\|_{L^2(Q)^{1+n}} + \|\varepsilon y_1\|_{L^2(\Omega)})$$

and so

$$\|g\|_{C([0,T];L^2(\Omega)^{1+n})} \leq \varepsilon K(\|y\|_X + \|y_1\|_{L^2(\Omega)}),$$

where K is a constant.

Hence, $y_\varepsilon \to y$ as $\varepsilon \to 0$. Next, we define $z = g/\varepsilon - w$. Then, it is required to prove that $z \to 0$ as $\varepsilon \to 0$. From the definition of z, we get

$$\begin{aligned} &\frac{\partial z}{\partial t} = Az + \sum_{i=1}^{m+2} u_i B_i z + \sum_{i=1}^{m+2} h_i B_i g \\ &\vec{n} \cdot (\nabla z_1 - \vec{u_b} \cdot z_1) = \vec{n} \cdot (\vec{h_b} g_1) \\ &z(0) = 0. \end{aligned} \tag{4.42}$$

Invoking Theorem 1.1, since $g \to 0$, we infer that $z \to 0$ as $\varepsilon \to 0$ and hence, $g/\varepsilon \to w$. $\square$

We now consider the reduced problem,

$$\min_{u \in U_{ad}} \hat{J}(u) := J(\Xi(u), u) \tag{4.43}$$

We define the formal adjoints $A^\#$ and $B_i^\#$,

$$A^\# = \begin{bmatrix} \nabla^2 & k_f & 0 \\ 0 & -k_f & 0 \\ 0 & 0 & 0 \end{bmatrix} \quad B_1^\# = \begin{bmatrix} -\frac{\partial}{\partial x_1} & 0 & 0 \\ 0 & 0 & 0 \\ 0 & 0 & 0 \end{bmatrix} \quad B_1^\# = \begin{bmatrix} \frac{\partial}{\partial x_1} & 0 & 0 \\ 0 & 0 & 0 \\ 0 & 0 & 0 \end{bmatrix} \quad B_2^\# = \begin{bmatrix} \frac{\partial}{\partial x_2} & 0 & 0 \\ 0 & 0 & 0 \\ 0 & 0 & 0 \end{bmatrix}$$

$$B_i^\# = \begin{bmatrix} -H_{i-2} & H_{i-2} & H_{i-2} \\ 0 & 0 & 0 \\ 0 & 0 & 0 \end{bmatrix} \quad 3 \leq i \leq k_f + 2 \tag{4.44}$$

These are defined as formal adjoints. This is so, as an actual representation of the adjoints of differential operators requires the definition of their domain, typically using boundary conditions. We will not need the adjoints of each of these operators but only their sum, i.e, $(A_0 + \sum_{i=1}^{m+2} h_i B_i)^*$. We do not take the adjoints of the summands to represent the adjoints of the sum. This is because for unbounded operators the equality between adjoints of sums and their summands does not hold in general. For more details refer to [Grubb (2008)].

Theorem 4.1.7. *The reduced objective functional $\hat{J}$ is differentiable in the Gateaux sense, and the derivative has the form*

$$\langle \hat{J}'(u), h\rangle_{L^2(0,T)^{m+2}} = \int_0^T \langle \vec{n}\cdot(\vec{h_b}p_1), y_1\rangle_{L^2(\partial\Omega)} + \int_0^T \langle \sum_{i=1}^{m+2} h_i B_i y, p\rangle_{L^2(\Omega)^{1+n}} + \lambda \langle u, h\rangle_{L^2(0,T)^{m+2}}, \tag{4.45}$$

where p is the solution of the backward-in-time adjoint equation,

$$\begin{aligned} -\frac{\partial p}{\partial t} &= A^{\#}p + \sum_{i=1}^{m+2} u_i B_i^{\#} p \\ \vec{n}\cdot\nabla p_1 &= 0 \\ p(T) &= W^*(Wy(\cdot,T) - y_\Omega). \end{aligned} \tag{4.46}$$

Proof. We use the generalized chain rule of differentiation of operators in Banach spaces to prove the above result.

Consider $G : C([0,T];L^2(\Omega)^{1+n}) \to L^2(\Omega)^{1+n}$, which maps the state to its final value. This linear continuous mapping is well-defined for functions in the domain $C([0,T];L^2(\Omega)^{1+n})$ due to continuity in time over a compact set.

Using the chain rule of differentiation,[Tröltzsch (2010)] [Pinnau and Ulbrich (2008)] (since $\hat{J}$ is Frechet differentiable and Ξ is Gaeteaux differentiable) the Gateaux derivative of $\hat{J}$ is given by

$$\langle \hat{J}'(u), h\rangle = \langle J_y(y,u), \Xi'(u)h\rangle + \langle J_u(y,u), u\rangle, \tag{4.47}$$

which is equal to

$$\langle \hat{J}'(u), h\rangle = \langle G^*W^*(WGy - y_\Omega), w\rangle + \lambda\langle u, h\rangle. \tag{4.48}$$

Thus we have,

$$\langle \hat{J}'(u), h \rangle = \langle W^*(WGy - y_\Omega), Gw \rangle + \lambda \langle u, h \rangle \tag{4.49}$$

Then,

$$\langle \hat{J}'(u), h \rangle = \langle p(\cdot, T), w(\cdot, T) \rangle + \lambda \langle u, h \rangle$$

Consider the term $\langle p(\cdot, T), w(., T) \rangle$. Using integration by parts in time, we find that this term is:

$$\int_0^T \langle \frac{\partial p}{\partial t}, w \rangle + \int_0^T \langle p, \frac{\partial w}{\partial t} \rangle + \langle p(0), w(0) \rangle$$

and hence is equal to:

$$\int_0^T \langle \frac{\partial p}{\partial t}, w \rangle + \int_0^T \langle p, A_0 w + \sum_{i=1}^{m+2} u_i B_i w + \sum_{i=1}^{m+2} h_i B_i y \rangle,$$

Let us now define the formal adjoints of these operators,

$$A_0^\# = \begin{bmatrix} M_0^\# & 0 & 0 \\ k_f & -k_f & 0 \\ 0 & 0 & 0 \end{bmatrix} \tag{4.50}$$

such that $M_0^\# : L^2(0,T;V) \to L^2(0,T;V^*)$ is given by

$$\left\langle M_0^\# y, \phi \right\rangle_{V^*,V} = -\langle D\nabla y, \nabla \phi \rangle_{L^2(\Omega)} \tag{4.51}$$

Equation 4.46 has a solution in the weak sense and,

$$-\langle \frac{\partial p}{\partial t}, \phi \rangle = \langle A_0^\# p, \phi \rangle + \sum_{i=1}^{m+2} \langle u_i B_i^\# p, \phi \rangle \tag{4.52}$$

for all $\phi \in L^2(0,T;X)$ The previous step can be written as,

$$\int_0^T \langle \frac{\partial p}{\partial t}, w \rangle + \int_0^T \langle A_0^\# p + \sum_{i=1}^{m} u_i B_i^\# p, w \rangle + \int_0^T \vec{n} \cdot (\vec{h_b} p y) + \int_0^T \langle p, \sum_{i=1}^{m+2} h_i B_i y \rangle.$$

It follows that

$$\langle p(\cdot, T), w(., T) \rangle = \int_0^T \int_{\partial\Omega} \vec{n} \cdot (\vec{h_b} p_1 y_1) + \int_0^T \langle p, \sum_{i=1}^{m} h_i B_i y \rangle,$$

and hence we have our result. □

The adjoint state equation for the system defined in Equation 2.4 with respect to the objective functional, J, is therefore given by:

$$\begin{aligned}
-\frac{\partial p_1}{\partial t} &= \nabla \cdot (D\nabla p_1 + \mathbf{v}(t)p_1) + \sum_{i=1}^{n_f} k_i H_i(-p_1 + p_2 + p_3) \ \ in \ \ Q, \\
-\frac{\partial p_2}{\partial t} &= k_f p_1 - k_f p_2 \ \ in \ \ Q, \\
-\frac{\partial p_3}{\partial t} &= 0 \ \ in \ \ Q,
\end{aligned} \tag{4.53}$$

with the Neumann boundary conditions

$$\vec{n} \cdot \nabla p_1 = 0 \ \ on \ \ \Sigma \tag{4.54}$$

and final time condition

$$p(T) = W^*(Wy(\cdot, T) - y_\Omega). \tag{4.55}$$

4.1.4 First Order Necessary conditions

Theorem 4.1.8. *Given the optimal control u^*, it satisfies the following condition,*

$$\langle J'(u^*), u^* - u \rangle \geq 0 \ \ \forall u \in U_{ad} \tag{4.56}$$

Proof. This follows from Equation 3.3. □

4.2 Mapping

In this section we analyze the mapping problem presented in section 1.3. Following is the macroscopic model for the mapping problem,

$$\begin{aligned}
\frac{\partial y_1}{\partial t} &= \nabla \cdot (D\nabla y_1 - \mathbf{v}(t)y_1) \quad in \ \ Q, \\
\frac{\partial y_2}{\partial t} &= k_o H y_1 \quad in \ \ Q,,
\end{aligned} \tag{4.57}$$

with the no-flux boundary conditions

$$\vec{\mathbf{n}} \cdot (D\nabla y_1 - \vec{\mathbf{v}}(t)y_1) = 0 \ \ on \ \ \Sigma. \tag{4.58}$$

H is a spatially dependent coefficient and models the presence or absence of a feature of interest in the environment. It is required that the spatial coefficient be reconstructed from some temporal information from robots regarding the number of observations made by them over time. More specifically the question of interest is whether the spatial coefficient, H can be reconstructed from $g(t) = \int_\Omega \frac{\partial y_2}{\partial t}(t)$ alone. The data, g, is collected from the agents, either from a stochastic simulation or an experiment. This section discusses the well posedness of the problem.

4.2.1 The Optimization Problem

It is required that we estimate an unknown spatial coefficient, $H \in S_{ad} \subset L^2(\Omega)$. Due to the one sided coupling between y_1 and y_2, the first state does not affect the solution of the estimation problem. Hence we can pose the problem as follows: We seek the solution of the system,

$$(KH)(t) = \int_\Omega k_o H(x) y_1(x,t) dx = g(t) \tag{4.59}$$

$$S_{ad} = \left\{ u \in L^2(\Omega); 0 \leq u(x) \leq 1 \;\; a.e \;\; x \in \Omega \right\} \tag{4.60}$$

The operator, $K : L^2(\Omega) \to L^2(0,T)$, is an integral operator. This type of equation is called a Fredholm integral equation of the first kind. Generally, Fredholm integral equations of the first kind need not have unique solutions, unless some special conditions on $k_o y_1(s,t)$, the kernal of the operator, can be guaranteed. To deal with ill-posedness of this inverse problem, it can be alternately posed as an optimization problem:

$$\min_{H \in S_{ad}} \;\; J(H) = \|KH - g\|^2_{L^2(0,T)} \tag{4.61}$$

In optimization parlance, this is a convex functional in H but not necessarily strictly convex.

4.2.2 Regularization, Differentiability and Sufficient Conditions

For unique solutions to the problem the functional can be made strictly convex as follows,

$$\min_{H \in S_{ad}} J_\lambda(H) = \frac{1}{2}\|KH - g\|^2_{L^2(0,T)} + \frac{\lambda}{2}\|H\|^2_{L^2(\Omega)} \tag{4.62}$$

for $\lambda > 0$. λ is called the regularization parameter and is quite often used in the so called, 'Tikohnov regularization' of inverse problems. The existence and uniqueness of the solution to this problem can be easily guaranteed. For details regarding existence and uniqueness of this problem one can refer to [Kirsch (2011)].

For the gradient descent method used later, we need a characterization of the derivative of the objective functional. The objective functional is differentiable in Frechet sense. Since $K \in \mathscr{L}(L^2(\Omega), L^2(0,T))$, derivative of K is itself. Then by chain rule of differentiation, the Frechet derivative of J_λ, $J'_\lambda(H)$ is given by,

$$\langle J'_\lambda(H), s\rangle_{L^2(\Omega)} = \langle KH - g, Ks\rangle_{L^2(0,T)} + \lambda\langle H, s\rangle_{L^2(\Omega)} \tag{4.63}$$

Using Reiz representation (Equation 3.1) we can get explicit representation of the derivative, ∇J_λ as,

$$\nabla J_\lambda = K^*(KH - g) + \lambda H \quad \in L^2(\Omega). \tag{4.64}$$

Here $K^* \in \mathscr{L}(L^2(0,T), L^2(\Omega))$ is given by,

$$(K^*G)(x) = \int_0^T k_o G(t) y_1(x,t)dt \quad \forall p \in L^2(0,T). \tag{4.65}$$

To verify that the characterization of K^* is correct it can easily be checked that,

$$\langle KH, G\rangle_{L^2(0,T)} - \langle H, K^*G\rangle_{L^2(\Omega)} = 0 \quad \forall H \in L^2(\Omega),\ \forall G \in L^2(0,T). \tag{4.66}$$

Chapter 5

NUMERICAL IMPLEMENTATION

5.1 PDE Simulation

This section describes the numerical algorithm used to approximate the solution of the primal and dual system of PDEs. Towards this end we use the method of lines(MOL) approach for numerical simulation. A detailed explanation of these approaches can be found in [Hundsdorfer and Verwer (2003)] [Leveque (2004)]. The MOL approach involves explicit discretization of the concerned operators and system variables in space. The variables are left continuous in time. The resulting semi-discretized system is system of ordinary differential equations(ODEs). The system of ODEs can then be solved numerically using any commericial ODE solver.

The spatial domain $\Omega = (0,1) \times (0,1)$ is approximated using a spatial discretized domain Ω_h. The n^{th} coordinate is discretized as $X_n = \{x_{n,-1}, x_{n,0} x_{n,1}, x_{n,2}, x_{n3} \ldots . x_{nm}, x_{n,m+1}\}$. Here $x_{nj} = jh$ and $h = 1/m$ is the mesh width. Then $\Omega_h = X_1 \times X_2$. The points $x_{n,-1}, x_{n,0}$ and $x_{n,m+1}$ are ghost points used to numerically define the boundary conditions of the system. Figure 5.1 is a visual depiction of a small section of the discretized domain.

Let y_1^{ij} denote an approximation to $y(x_{1i}, x_{2j})$. The spatial discretisation of the Laplacian operator, $\nabla^2 \cdot$ is given by

$$\nabla_h^2 y_1^{ij} = \frac{1}{h^2}(y_1^{i-1,j} + y_1^{i+1,j} + y_1^{i,j-1} + y_1^{i,j+1} - 4y_1^{ij}) \tag{5.1}$$

Straightforward finite difference discretization of the advection operator can lead to spurious oscillations in the numerical solution. To deal with such issues we use a flux limiter

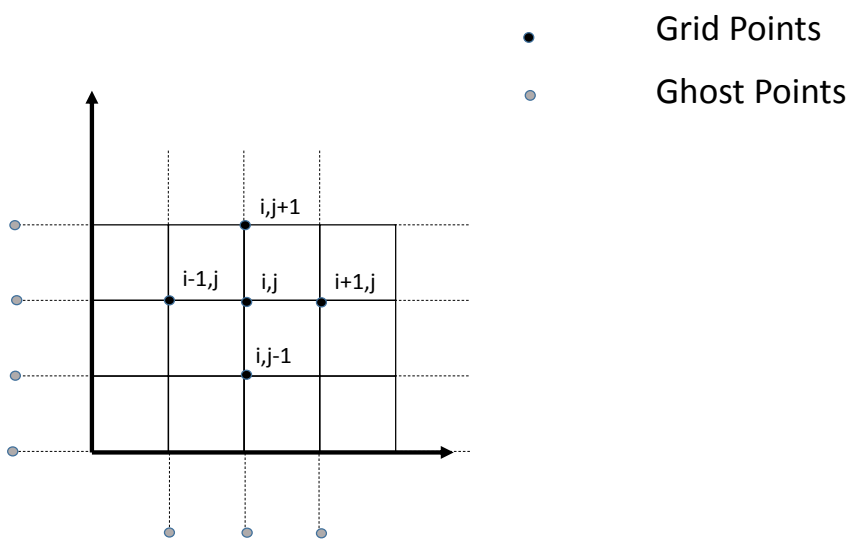

Figure 5.1: Sample numerical grid

based approximation. Advection in the x_1 and x_2 directions are approximated as

$$\begin{aligned} v_{x_1}(t)\frac{\partial_h y_1^{ij}}{\partial x}(t) &= v_{x_1}(t)\frac{1}{h}\left(f^{i-\frac{1}{2},j}(t,y_1(t)) - f^{i+\frac{1}{2},j}(t,y_1(t))\right) \\ v_{x_2}(t)\frac{\partial_h y_1^{ij}}{\partial x}(t) &= v_{x_2}(t)\frac{1}{h}\left(f^{i,j-\frac{1}{2}}(t,y_1(t)) - f^{i,j+\frac{1}{2}}(t,y_1(t))\right) \end{aligned} \tag{5.2}$$

The flux term, $f(t,y_1(t))$ can be given in a general form as

$$\begin{aligned} f^{i+\frac{1}{2},j}(t,y_1) &= v_{x_1}(t)\left[y_1^{i,j} + \psi(\theta^i)(y_1^{i+1,j} - y_1^{i,j}), \quad v_{x_1}(t) \geq 0,\right. \\ f^{i+\frac{1}{2},j}(t,y_1) &= v_{x_1}(t)\left[y_1^{i,j} + \psi(\theta^j)(y_1^{i+1,j} - y_1^{i,j})\right] \quad v_{x_2}(t) \geq 0, \\ f^{i+\frac{1}{2},j}(t,y_1) &= v_{x_1}(t)\left[y_1^{i+1,j} + \psi(\frac{1}{\theta^{i+1}})(y_1^{i,j} - y_1^{i+1,j})\right], \quad v_{x_1}(t) < 0, \\ f^{i+\frac{1}{2},j}(t,y_1) &= v_{x_1}(t)\left[y_1^{i,j+1} + \psi(\frac{1}{\theta^{j+1}})(y_1^{i,j} - y_1^{i,j+1})\right], \quad v_{x_2}(t) < 0, \end{aligned} \tag{5.3}$$

Here, θ_i and θ_j are ratios given by,

$$\begin{aligned} \theta^i &= \frac{y_1^{i,j} - y_1^{i-1,j}}{y_1^{i+1,j} - y_1^{i,j}}] \\ \theta^j &= \frac{y_1^{i,j} - y_1^{i,j-1}}{y_1^{i,j+1} - y_1^{i,j}} \end{aligned} \tag{5.4}$$

ψ is called the limiter function. We use the superbee flux limiter which has the following form,

$$\psi(r) = max\,[0, min(2r,1), min(r,2)] \tag{5.5}$$

Note that the above implementation results in a nonlinear discretization for the originally linear system.

For the implementation of boundary conditions the following numerical values are assumed at the ghost points,

$$\begin{aligned} y_1^{m+2,j} &= 0 \quad -1 \le j \le m+2 \\ y_1^{i,m+2} &= 0 \quad -1 \le i \le m+2 \\ y_1^{-1,j} &= 0 \quad -1 \le j \le m+2 \\ y_1^{i,-1} &= 0 \quad -1 \le i \le m+2 \end{aligned} \tag{5.6}$$

The zero flux boundary condition, Equation 2.5, can then be implemented based on a simple reflection as

$$\begin{aligned} \frac{dy_1^{m,j}}{dt} &= \frac{dy_1^{m+1,j}}{dt} + \frac{dy_1^{m,j}}{dt}, \quad 0 \le j \le m+1 \\ \frac{dy_1^{m+1,j}}{dt} &= 0, \quad 0 \le j \le m+1 \\ \frac{dy_1^{i,m}}{dt} &= \frac{dy_1^{i,m+1}}{dt} + \frac{dy_1^{i,m}}{dt}, \quad 0 \le i \le m+1 \\ \frac{dy_1^{i,m+1}}{dt} &= 0, \quad 0 \le i \le m+1 \\ \frac{dy_1^{1,j}}{dt} &= \frac{dy_1^{0,j}}{dt} + \frac{dy_1^{1,j}}{dt}, \quad 0 \le j \le m+1 \\ \frac{dy_1^{0,j}}{dt} &= 0, \quad 0 \le j \le m+1 \\ \frac{dy_1^{i,1}}{dt} &= \frac{dy_1^{i,0}}{dt} + \frac{dy_1^{i,1}}{dt}, \quad 0 \le i \le m+1 \\ \frac{dy_1^{i,0}}{dt} &= 0, \quad 0 \le i \le m+1 \end{aligned} \tag{5.7}$$

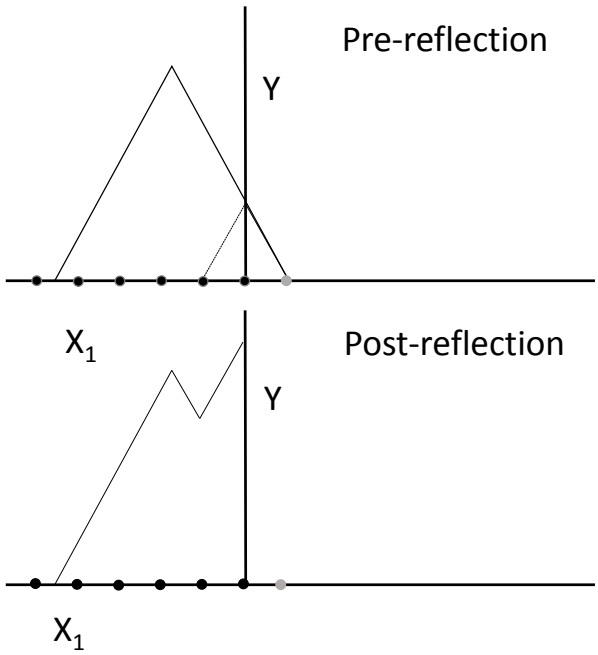

Figure 5.2: The zero flux boundary condition for a 1 dimensional cross-ection

Figure 5.2 is a visual depiction of the zero flux boundary condition implemented as a reflection.

The numerical approximation for the adjoint system, Equation 4.53, Equation 4.54 and Equation 4.55, is done in a similar manner. However, the adjoint system does not have a zero flux boundary condition, but Neumann boundary conditions. The rectangular domain implies that $\vec{n} \cdot \nabla p_1 = 0$ reduces to $\frac{\partial p_1}{\partial x_1} = 0$ and $\frac{\partial p_1}{\partial x_2} = 0$ on edges parallel to the x_1 and x_2 co-ordinate axes respectively. The first derivatives can be approximated as

$$\begin{aligned} \frac{\partial p_1^{ij}}{\partial x_1} &= \frac{1}{h}\left(p_1^{i+1,j} - p_1^{i,j}\right) \\ \frac{\partial p_1^{ij}}{\partial x_2} &= \frac{1}{h}\left(p_1^{i,j+1} - p_1^{i,j}\right) \end{aligned} \tag{5.8}$$

or

$$\begin{aligned} \frac{\partial p_1^{ij}}{\partial x_1} &= \frac{1}{h}\left(p_1^{i,j} - p_1^{i-1,j}\right) \\ \frac{\partial p_1^{ij}}{\partial x_2} &= \frac{1}{h}\left(p_1^{i,j} - p_1^{i,j-1}\right) \end{aligned} \tag{5.9}$$

Equation 5.8 and Equation 5.9 are the forward and backward first-order finite difference approximations of the first derivative of a function, respectively. Then the Neumann boundary conditions can be implemented numerically by making the following substitutions,

$$\begin{aligned} p_1^{m+1,j} &= p_1^{m,j} \quad 0 \leq j \leq m+1 \\ p_1^{i,m+1} &= p_1^{i,m} \quad 0 \leq i \leq m+1 \\ p_1^{0,j} &= p_1^{1,j} \quad 0 \leq j \leq m+1 \\ p_1^{i,0} &= p_1^{i,1} \quad 0 \leq i \leq m+1 \end{aligned} \tag{5.10}$$

The zero flux boundary condition was not implemented using the method outlined above for neumann boundary conditions. This was due to the excessive numerical diffusion experienced at the boundaries because of the nature of the boundary condition. Due to the high advection in the system, the solution results in sharp increase in the spatial derivatives of the states near the boundaries. This is typical of singularly perturbed ADR equations. An alternative method of implementation is the use of non-uniform grids (as in [Roos *et al.* (2008)]), where the grid is taken to be finer near the boundaries to enable better approximation in regions of sharp transitions.

5.2 Optimization Algorithm

We use the projected gradient method to approximate the optimal controls iteratively. We start with the initial arbitrary estimation of the optimal control u_0. Let $\mathbb{P}_C(x)$ denote the projection of x on the set C. Then the algorithm can be stated as follows,

Algorithm 5.2.1. *Projected Gradient Method*

1. *Find the solution, y_n, corresponding to the state system Equation 2.4 with $u = u_n$*

2. *Solve the adjoint states, p_n, with $u = u_n$ and $y = y_n$.*

3. *Take new descent direction using Equation 4.45 as*

$$w_n = -\hat{J}'(u_n) \tag{5.11}$$

4. *Compute step size vector, $\vec{\alpha}$, using a line search (an example is defined below) on the projected gradient, using the control constraints, u_a and u_b so that,*

$$\hat{J}(\mathbb{P}_{[u_a,u_b]}(u_n + \vec{\alpha}_n w_n)) \geq \hat{J}(u_n) \tag{5.12}$$

5. *Set $u_{n+1} = \mathbb{P}_{[u_a,u_b]}(u_n + \vec{\alpha}_n w_n)$*

6. *if $\hat{J}(u_{n+1}) - \hat{J}(u_n) > -\beta$ set $n = n+1$ and Goto 1*

At step 4 a possible step size needs to be identified, to find a suitable value of the each of the elements, α_n^k, of the step size vector, $\vec{\alpha}_n$, so that the new descent step, u_{n+1}, achieves a useful reduction in the value of the objective function.

For the mapping problem the optimization algorithm is very similar except that at the 3rd step we use Equation 4.64. And instead of $[u_a, u_b]$ we project over S_{ad} as in Equation 4.60.

Algorithm 5.2.2. *Line search*

1. *Choose some $\gamma_1 \in \mathbb{R}$ such that $0 < \gamma_1 < 1$.*

2. *Choose some $\gamma_{2,1} \in \mathbb{R}$ such that $0 < \gamma_{2,1} \leq 1$ and set $j = 1$.*

3. *Evaluate $S = \hat{J}(\mathbb{P}_{[u_a,u_b]}(u_n^1, u_n^2 ... (u_n^k + \gamma_{2,j} w_n^k)) ...) - \hat{J}(u_n)$.*

4. *If $S > 0$ and $j < 10$ then set $j = j+1$, $\gamma_{2,j+1} = \gamma_1 \gamma_{2,j}$ and Goto 3.*

5. *Set $\alpha_n^k = \gamma_{2,j}$.*

5.3 Stochastic Simulation Algorithm

This section describes the algorithm used for the simulation of the microscopic models. The time interval, $[0,T]$, is discretized over a uniform grid, and the agent states are computed at time $t = i\Delta t$ for $i = 1,2,3....N_t$, where $\Delta t = T/N_t$ is the size of each time interval. The controls u are taken to be piece wise linear over these time intervals. The variable s_j stores the current state of agent j: $s_j = 0$ if the agent is flying, and $s_j = 1$ if the agent is hovering. Then the following is the numerical algorithm used to simulate an agent,

Algorithm 5.3.1. *Stochastic Simulation*

1. *Initialize* $t = 0, s_j = 0$;
2. $t = t + \Delta t$;
3. *If* $s_j = 0$*, then generate a random vector* $\vec{Z}$ *from a normal distribution with mean* 0 *and standard deviation* 1 *and set* $\vec{x_j} = \vec{x_j} + (2D\Delta t)^{1/2}\vec{Z} + \vec{v}(t)\Delta t$.
4. *Generate a random number* r_j *uniformly distributed in the interval* $(0,1)$.
5. *if* $s_j = 0$*,* $r_j \leq H_m(\vec{x_j})k_m(t)\Delta t$ *then* $s_j = 1$ *and Goto 7.*
6. *if* $s_j = 1$ *and* $r_j \leq k_f \Delta t$ *then* $s_j = 0$.
7. *if* $t < T$ *then Goto* 2.

m denotes the flower type and hence step 5 should be repeated for each m if the number of flower types is more than m.

Chapter 6

SIMULATION RESULTS

6.1 Planning and Allocation Problem

We developed microscopic and macroscopic models of scenarios in which a swarm of robots is tasked to achieve a specified spatial distribution of flower visits over five crop rows. We considered four different scenarios. We computed optimal control parameters of the macroscopic model to achieve two types of target spatial distributions of visits over the crop rows: one in which visits were required throughout the entire domain (*Objective 1*), and another in which they were required only on part of the domain (*Objective 2*). For both objectives, we simulated an environment with and without obstacles to investigate the effect of the geometry on the optimized robot control policies.

For each scenario, we simulated 1000 robots over a domain for size 100 m $\times$ 100 m. We set $k_f = 0.2s^{-1}$ to define an expected pollination time of $k_f^{-1} = 5$ s. In the optimization, the robot speed was bounded between -0.1 and 0.1 m/s, and the transition rates k_j were bounded between 0 and 1.25 s^{-1}. The microscopic model was simulated over a grid of 21×21 cells. To account for numerical diffusion, the partial differential equation was simulated over a finer grid of 51×51 cells. The diffusion coefficient, D, was taken to be $5 \times 10^{-4} m^2/s$. The terminal time, T was taken to be $480s$ for objective 1 and $100s$ for objective 2. Figure 6.1 shows three snapshots of the simulation of the stochastic agent based model for the case with *Objective 2* and obstacles.

In Objective 1, the error norm between the actual and target spatial distribution of flower visits was minimized. In Objective 2, the time until achieving the target distribution is minimized. Figure 6.2 shows that in all four scenarios, our optimal control approach success-

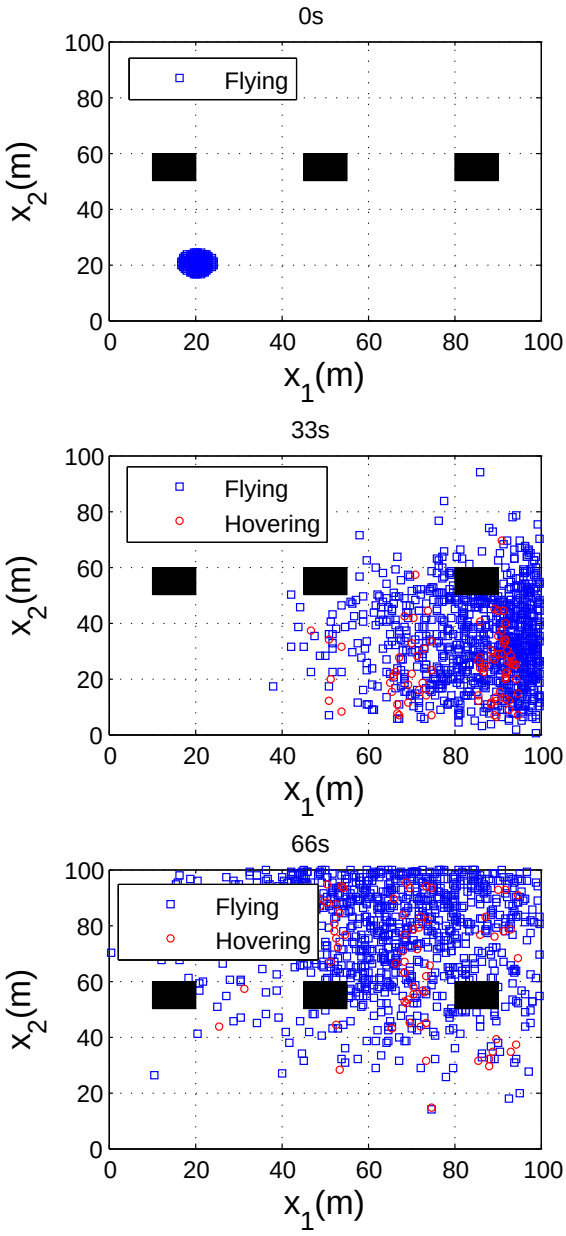

Figure 6.1: Particle state evolution over time

fully minimizes the objective function, driving it nearly to zero in the time span allotted for the simulation.

The resulting optimized parameters over time are plotted in Figure 6.3, with each of the two plots showing the parameter set for environments both with and without obstacles. The top plot of Figure 6.3 corresponds to the Objective 1 case, in which crops rows 2 and 4 were assigned twice as high a target density of flower visits as rows 1, 3, and 5. The robots start

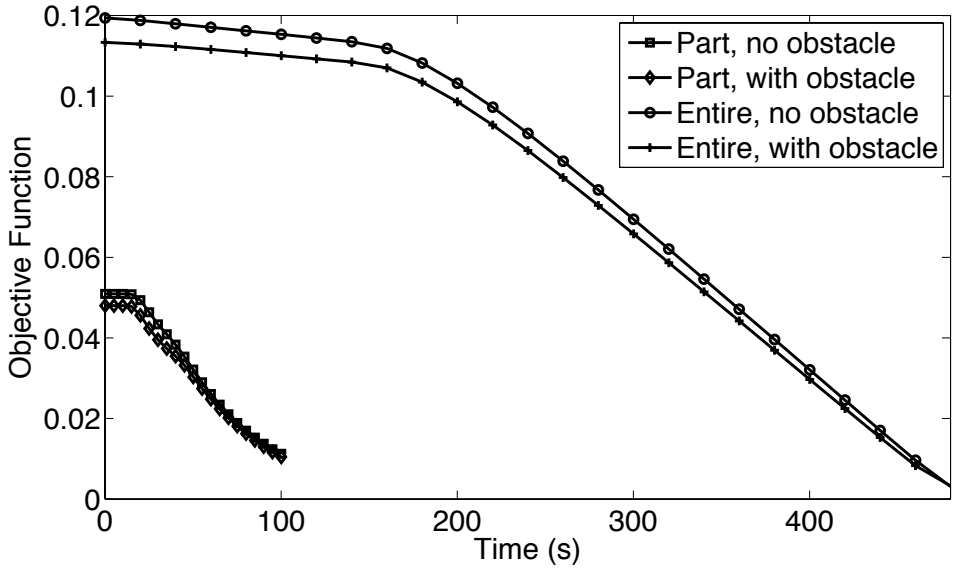

Figure 6.2: Objective function over time for all four scenarios

at the bottom of the field in this case. The robot speed is kept almost at zero throughout the optimization run; the robots' motion is dominated by diffusion, and after they diffuse over the entire domain (at 150 s), the transition rates are increased to approximately constant levels. The transition rate k_2, implemented when a robot is over row 2 or 4, is driven to about the twice the value of k_1, implemented for rows 1, 3, and 5, which results in twice as many flower visits over rows 2 and 4. The bottom plot of Figure 6.3 corresponds to the Objective 2 case, in which the target visit density is set to zero in rows 1, 2, and 3 and to a nonzero value in rows 4 and 5 (the rightmost two rows). In this case, the robots started at the left of the field, and their optimized speed in the positive x direction is kept high to drive them quickly to the right of the field. The transition rate k_1 increases as the robots slow down in the x direction, causing them to focus the bulk of their flower visits on the rightmost two rows.

Figure 6.4 through Figure 6.7 compare snapshots of the microscopic simulations (left columns) and macroscopic model numerical solutions (right columns) for each scenario. The two models are approximately similar in each case, which validates the ability of our

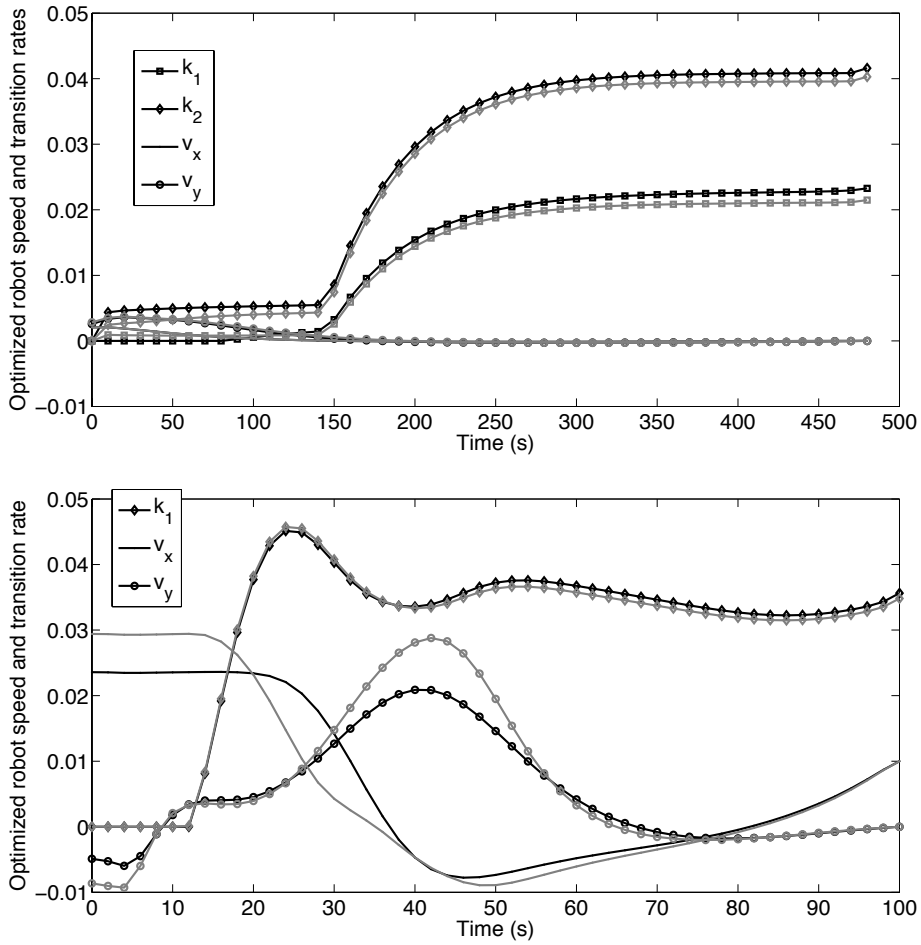

Figure 6.3: Optimized robot parameters for Objective 1 (top) and Objective 2 (bottom)

macroscopic model to predict the behavior of an ensemble of individual robots. The presence of obstacles in the domain does not significantly affect the progress of the robots for Objective 1, but it does impede their progress for Objective 2.

6.2 Mapping

We considered two cases to validate the Mapping approach proposed in the previous chapters. The first case was motivated by the pollination scenario considered for the planning and allocation problem. The second case was chosen arbitrarily. 30 agents were used in the stochastic simulation. The agents start about the point $(10, 10)$ as a gaussian distribu-

tion. The trajectories of the agents' were assigned by choosing appropriate velocity based controls, $\vec{v}$. These were chosen such that coverage of sufficient portion of the domain could be achieved. The sample trajectory of a single agent is shown in Figure 6.8. The diffusion coefficient was chosen to be $D = 1 \times 10^{-4} m^2/s$. The reaction rate, k_o, was assumed to be $100 s^{-1}$, that is high probability of registering a observation, when an agent passed over a region of interest. High reaction rates were needed to estimate the coefficient to sufficient accuracy with the proposed approach. The trials were simulated for the terminal time $T = 400s$.

The results of the first case are shown in Figure 6.9. The coefficient has been reconstructed to considerable accuracy. The error is the absolute error between the estimated coefficient and the actual one. The errors in approximation correspond to the edges of the features. This is typical of such methods familiar in image processing literature. The results of the second case are shown in Figure 6.10. As in the previous case the spatial coefficient has been reconstructed to considerable accuracy. The errors of approximation are highest along the edges of the features. The higher inaccuracy of the feature closer to the top edge can be attributed to the extensive diffusion experienced by the swarm as they reach this portion of the domain.

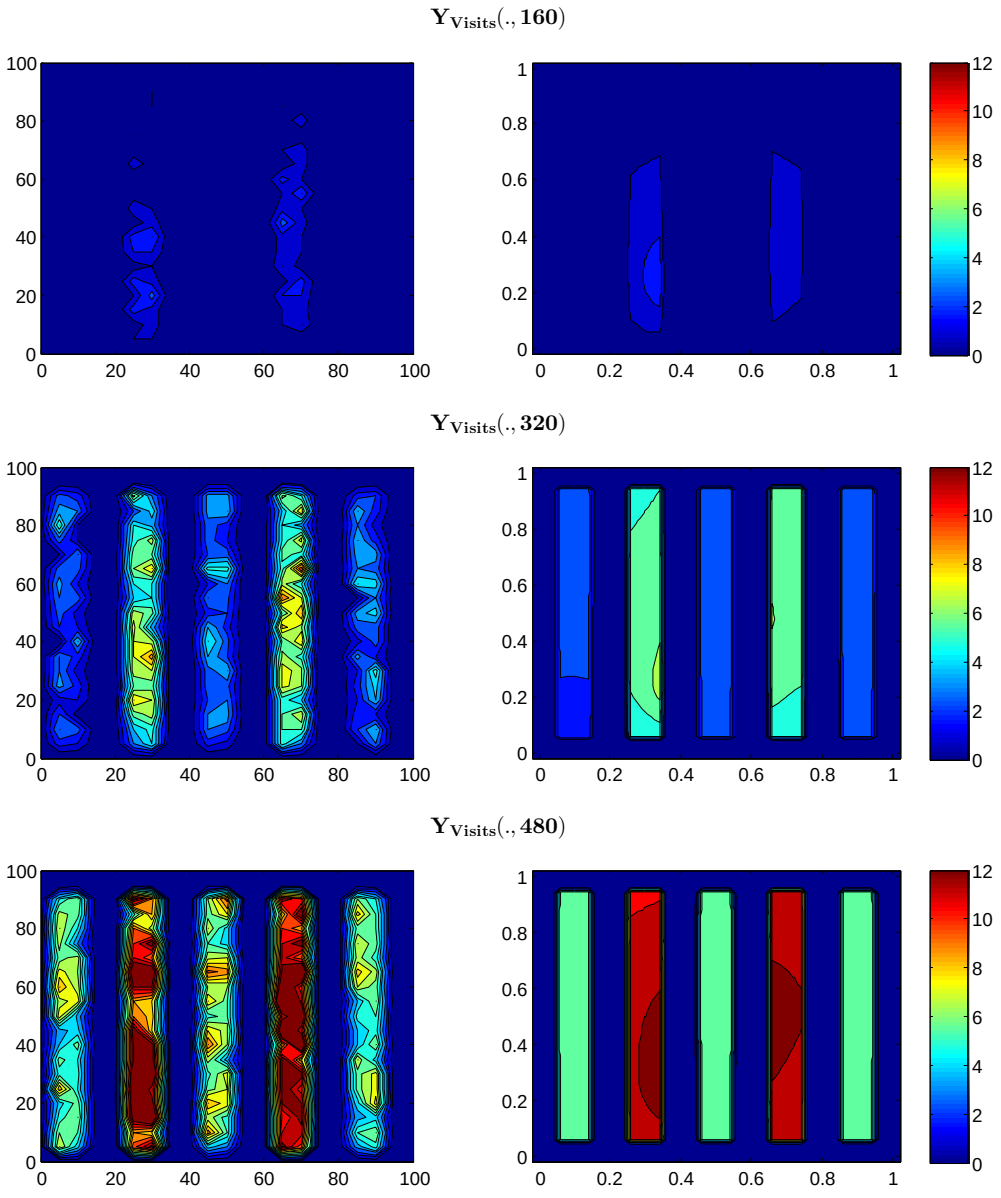

Figure 6.4: Distribution of flower visits at three times in the microscopic (left) and macroscopic (right) models with parameters optimized for Objective 1, no obstacles

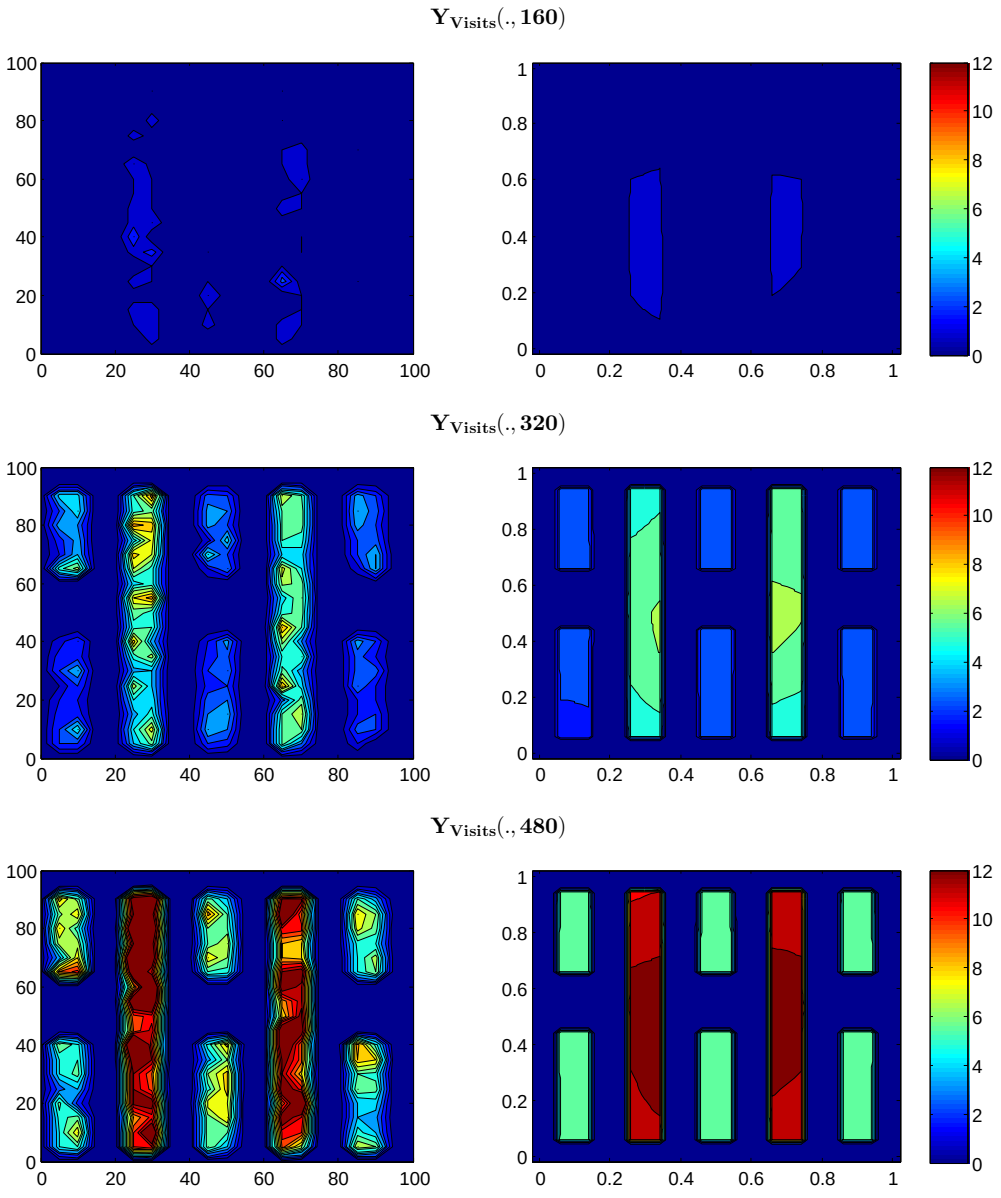

Figure 6.5: Distribution of flower visits at three times in the microscopic (left) and macroscopic (right) models with parameters optimized for Objective 1, with obstacles

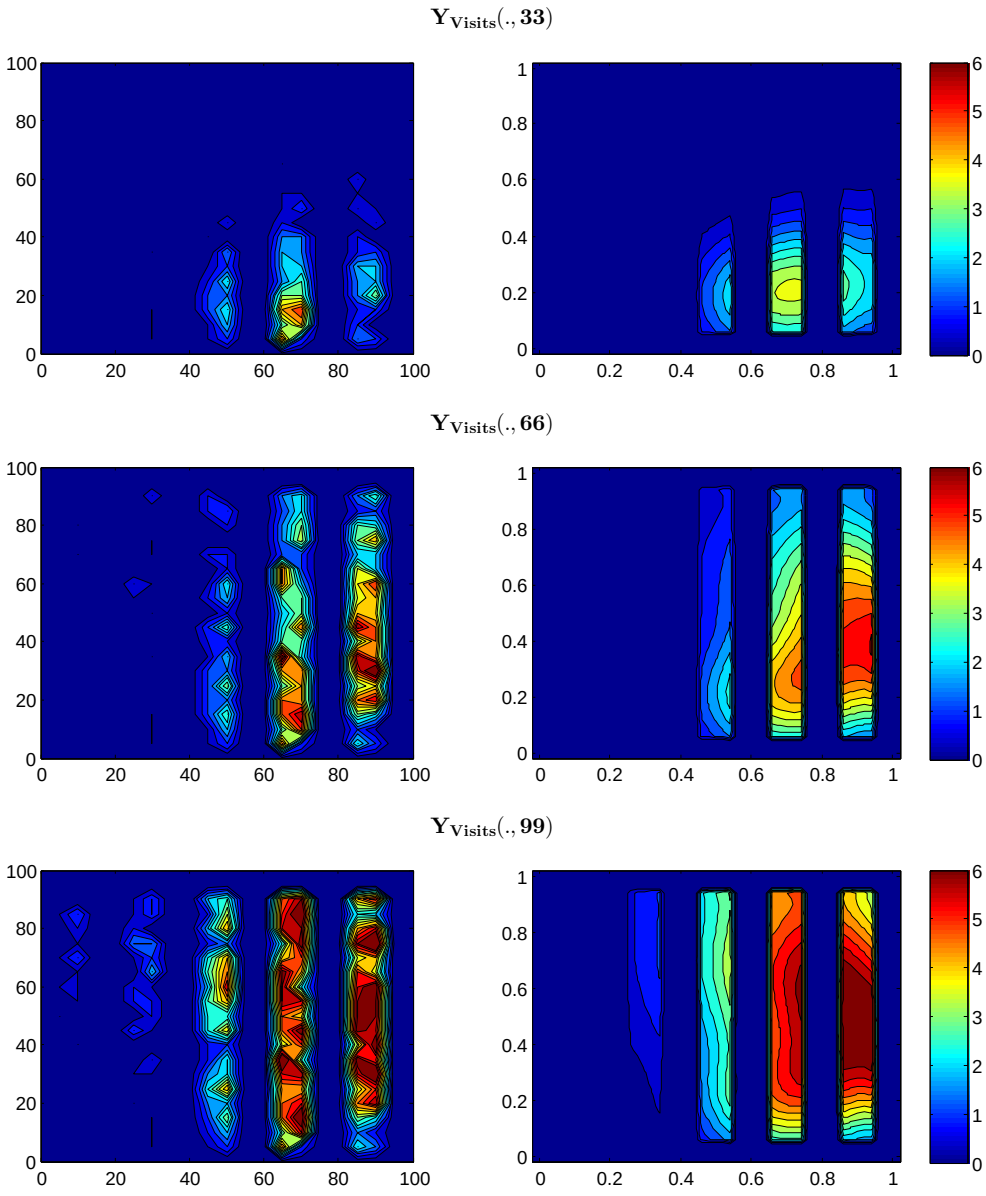

Figure 6.6: Distribution of flower visits at three times in the microscopic (left) and macroscopic (right) models with parameters optimized for Objective 2, no obstacles

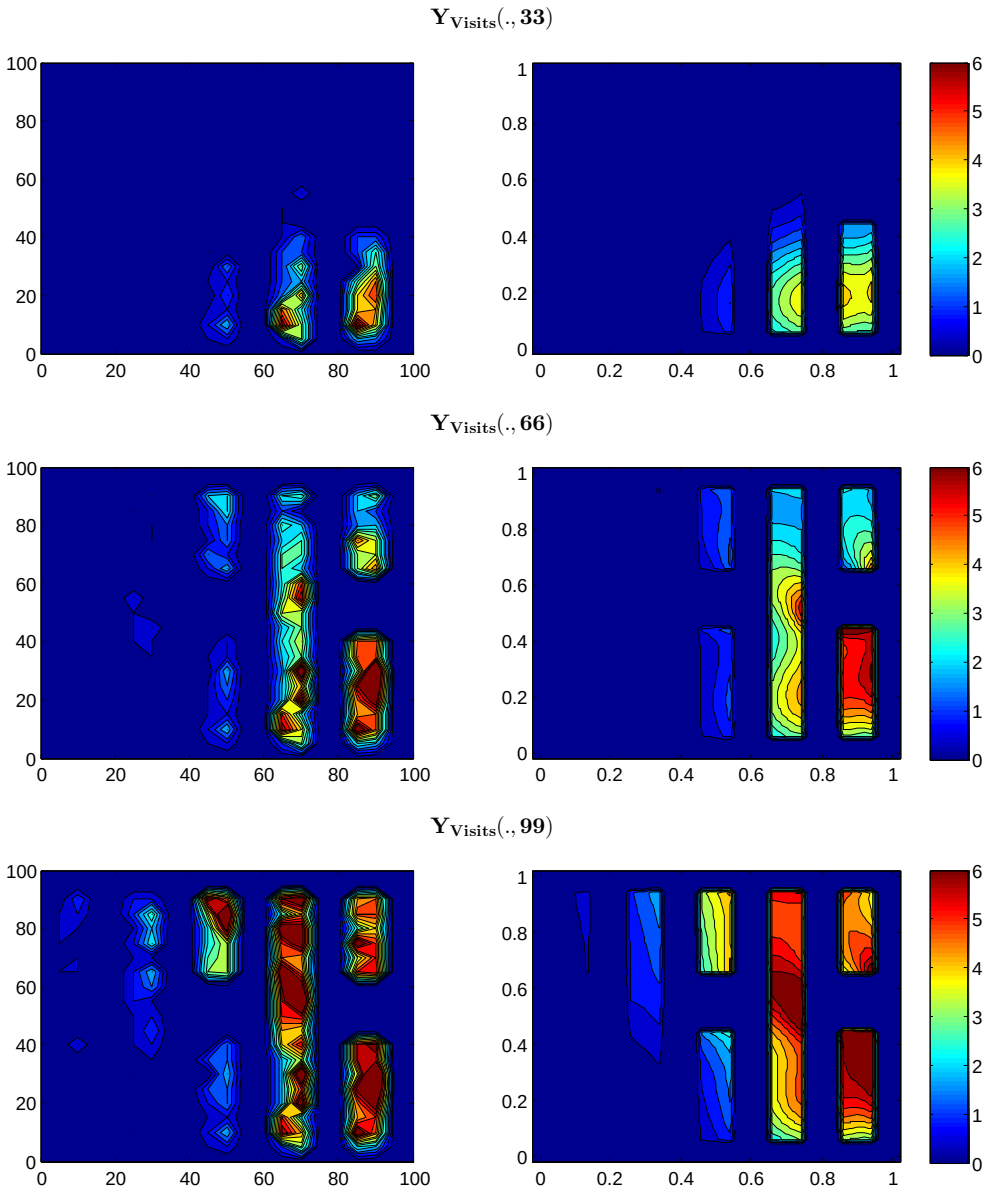

Figure 6.7: Distribution of flower visits at three times in the microscopic (left) and macroscopic (right) models with parameters optimized for Objective 2, with obstacles

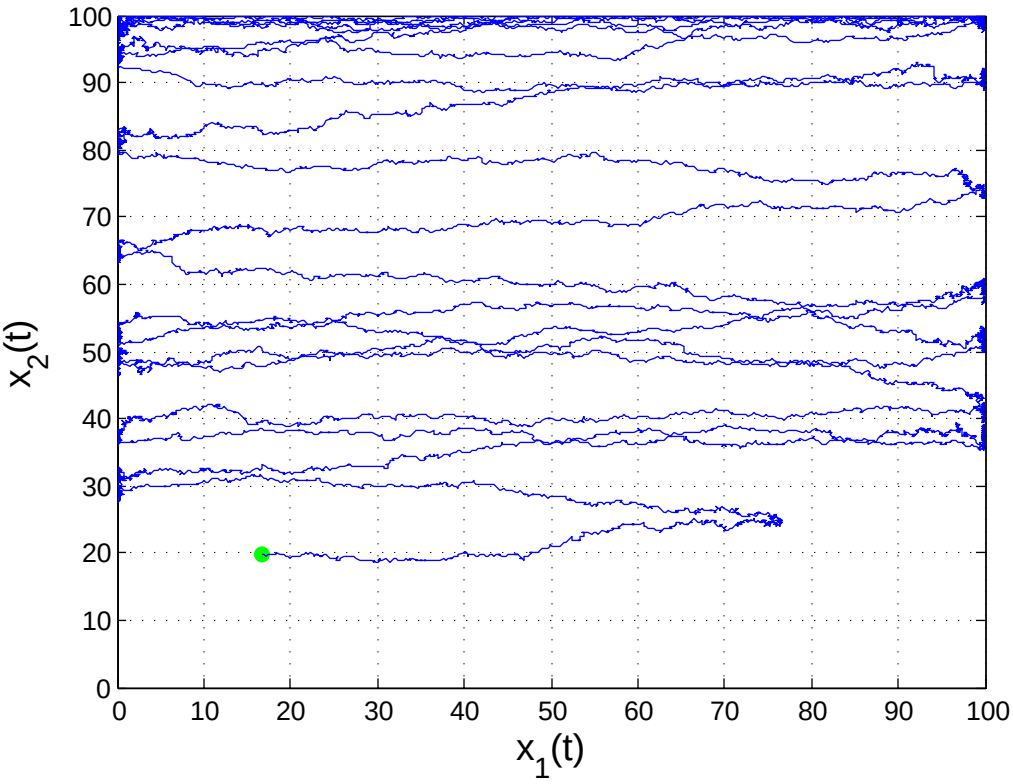

Figure 6.8: Trajectory of a single agent in lawn mower fashion for the mapping problem. The agent starts at the green dot.

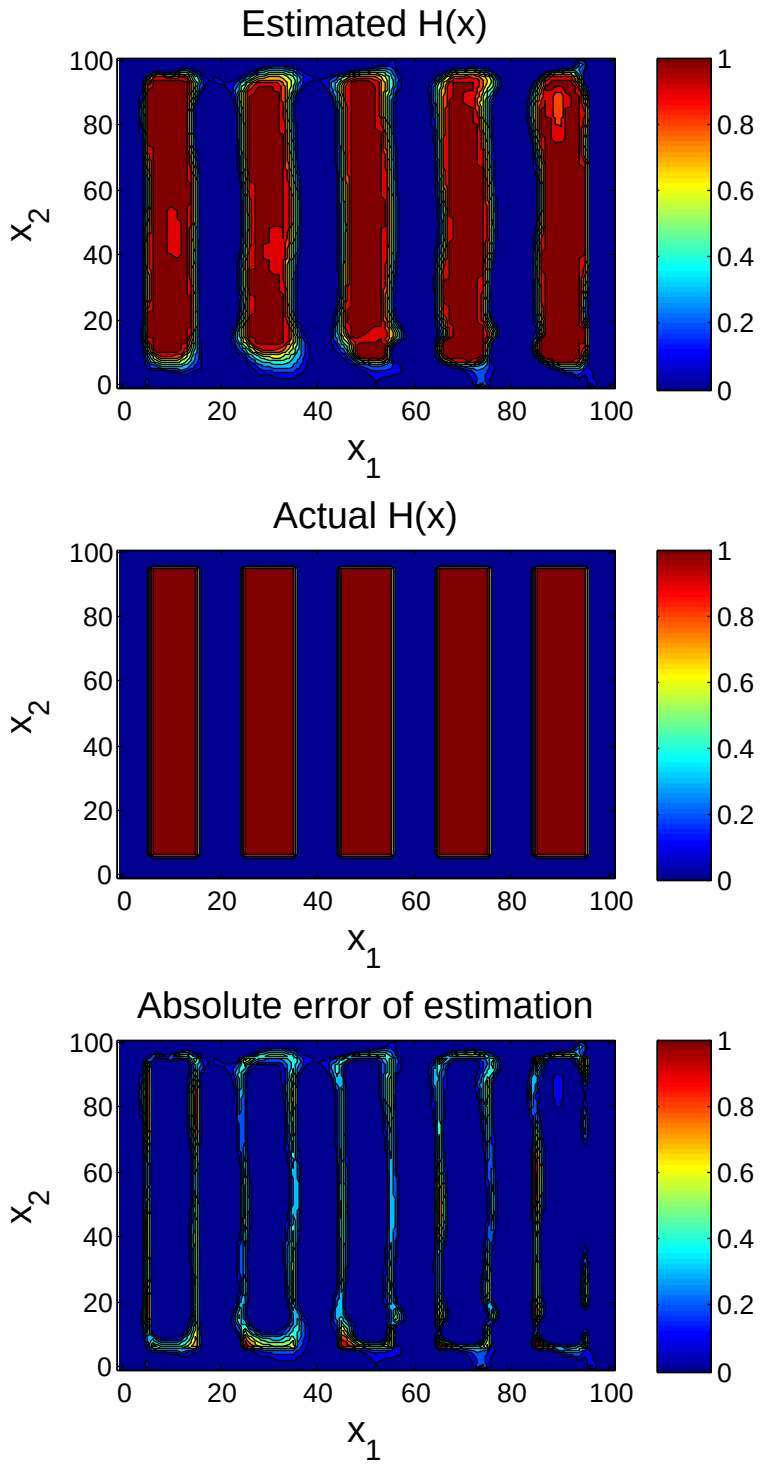

Figure 6.9: Estimated coefficient, H(x), for Case 1

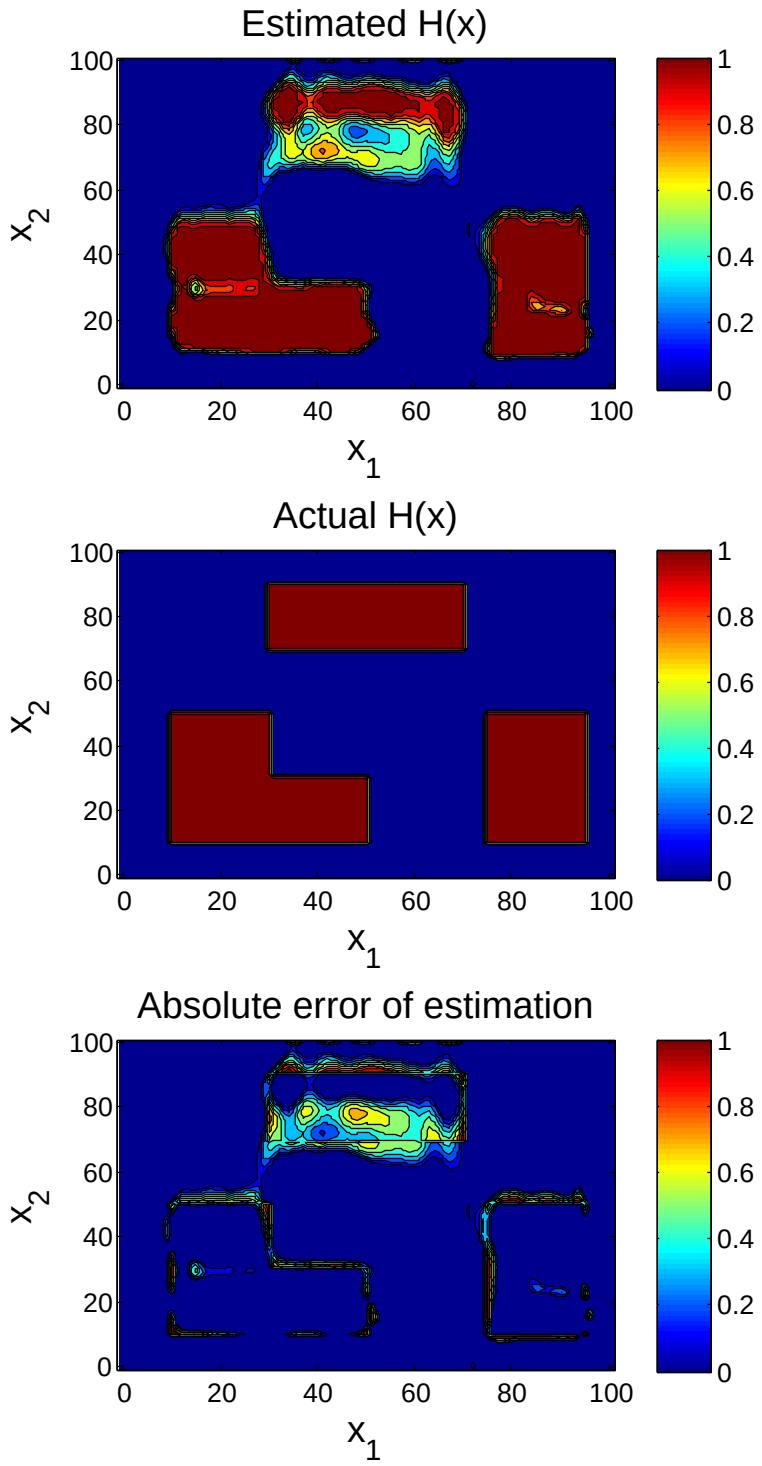

Figure 6.10: Estimated coefficient, H(x), for Case 2

Chapter 7

CONCLUSION

7.1 Summary of Contributions

This thesis presented an optimal control approach to the trajectory planning and task allocation problem for a swarm of diffusing and advecting robots that perform stochastic task transitions. The approach was used to realize efficient numerical algorithms for the synthesis of the resulting control inputs for the swarm. Additionally a mapping problem was analyzed and a method for feature reconstruction from robot observations was presented. The deterministic(PDE) model of the agent behavior enables the method to be robust to noisy motion of the agents.

7.2 Future Work

In order to guarantee robust behavior of the swarm one can consider the control strategies that are able to incorporate feedback from the robots in order to to fulfill a planning and allocation task in the presence of unknown environmental disturbances, say for example, as wind in the pollination scenario. For such scenarios, we must identify types of observers with minimal measurement costs that will provide sufficiently rich state reconstruction to enable real-time control in a broadcast control framework. As is often the case for infinite-dimensional systems, exact observability will not be possible unless all agents communicate back their state estimates. Some related work on industrial processes with similar controls has been done in [Vries *et al.* (2008)]. There has been very little work on stabilizability of bilinear infinite dimensional systems in general. This would be an opportunity from a control theoretical point of view and also relevant for the models used for

swarms as in this thesis. Another issue not addressed in this work is the degree of correspondence between the microscopic and the macroscopic models. It would be useful to study the kind of convergence that can be expected between the models and the relevance of the approach for the different regimes of swarm operation (for example, in terms of the number of agents in the swarm). Finally, we can expand the types of control schemes that we consider to include ones with inter-agent interactions, which is a common feature in PDE models of natural coordinated behaviors such as flocking, schooling, and taxis. These types of models introduce more non-linearities in the system description, which can make the control theory more challenging. In this regard, there is also some opportunity for work on modeling of large homogenous networks using PDEs. A leader induced formation control using boundary control of a PDE was considered in this direction [Elamvazhuthi and Berman (2014)]. However, more opportunities remain in terms non-linear hyperbolic PDEs for multiple formation using the same controller, infinite dimensional chains of non-holonomic agents, obstacle avoidance using these models. etc.

For the mapping problem, one could consider scenarios in which the topology of the domain is not known. However, such a problem necessarily introduces additional complexities in that the state space itself, which determines the domain of the PDE, needs to be estimated from the robot data. Hence the optimization problem would be to find the right state space. Moreover, assignment of agent trajectories becomes more challenging as an arbitrary trajectory might not ensure complete coverage of the unknown domain. A relevant problem in this regard is the famous problem posed by Mark Kac, "Can one hear the shape of a drum?" [Kac (1966)]. This problem is related to understanding the nature of evolution equations such as the wave equation and the diffusion equation over different geometries and the possibility of inferring the nature of this geometry from properties of the associated differential operators. A similar scenario could be considered in the mapping scenario where agents with stochastic dynamics return with some information that relates to the

spectrum of the differential operators associated with the PDE models. This could then be used subsequently to reconstruct the geometry of the domain. The application of geometric methods is an emerging theme in the control of PDEs [Croke (2004)]. Additionally, one could consider more efficient algorithms that do not require high probabilities of successful observations (and therefore high reaction rates) and hence are more tolerant to errors in the observations. In this regard one could consider compressed sensing approaches to mapping where rich information can obtained from relatively sparse data [Lustig *et al.* (2007)]. It would also be interesting to integrate the mapping and the planning-allocation phase of the swarm operation, where mapping is done first by a number of small, but highly capable swarm of explorer agents, followed by planning and allocation to larger swarm of agents based on the constructed map of the environment.

REFERENCES

Ball, J. M., J. E. Marsden and M. Slemrod, "Controllability for distributed bilinear systems", SIAM Journal on Control and Optimization **20**, 4, 575–597 (1982).

Beauchard, K. and J.-M. Coron, "Controllability of a quantum particle in a moving potential well", Journal of Functional Analysis **232**, 2, 328–389 (2006).

Becker, A., C. Onyuksel and T. Bretl, "Feedback control of many differential-drive robots with uniform control inputs", in "Intelligent Robots and Systems (IROS), 2012 IEEE/RSJ International Conference on", pp. 2256–2262 (IEEE, 2012).

Belmiloudi, A., *Stabilization, optimal and robust control: Theory and Applications in Biological and Physical Sciences* (Springer, 2008).

Berman, S., V. Kumar and R. Nagpal, "Design of control policies for spatially inhomogeneous robot swarms with application to commercial pollination", in "Int'l. Conf. Robotics and Automation (ICRA)", pp. 378–385 (2011a).

Berman, S., R. Nagpal and Á. Halász, "Optimization of stochastic strategies for spatially inhomogeneous robot swarms: A case study in commercial pollination", in "Int'l. Conf. Intelligent Robots and Systems (IROS)", pp. 3923–3930 (2011b).

Boulerhcha, M., B. Abdelhaq and L. Samir, "Optimal bilinear control problems governed by evolution partial differential equation", Int'l. Journal of Math. Analysis **6**, 2385–2395 (2012).

Casas, E. and D. Wachsmuth, *Second Order Optimality Conditions for Bang-bang Bilinear Control Problems* (Inst. of Math., 2014).

Croke, C. B., *Geometric methods in inverse problems and PDE control*, vol. 137 (Springer, 2004).

Elamvazhuthi, K. and S. Berman, "Scalable formation control of multi-robot chain networks using a pde abstraction", in "Int'l. Symp. on Distributed Autonomous Robotic Systems (DARS)", (Daejeon, Korea, 2014).

Elamvazhuthi, K. and S. Berman, "Optimal control of stochastic coverage strategies for robotic swarms", in "Proc. Int'l. Conf. on Robotics and Automation (ICRA)", (Seattle, WA, 2015), submitted.

Elliott, D., *Bilinear control systems* (Springer, 2009).

Evans, L. C., "Partial differential equations", (1998).

Fattorini, H. O., *Infinite dimensional optimization and control theory*, vol. 54 (Cambridge University Press, 1999).

Finotti, H., S. Lenhart and T. Van Phan, "Optimal control of advective direction in reaction-diffusion population models.", Evolution Equations & Control Theory **1**, 1 (2012).

Foderaro, G., *A Distributed Optimal Control Approach for Multi-agent Trajectory Optimization*, Ph.D. thesis, Duke University (2013).

Galstyan, A., T. Hogg and K. Lerman, "Modeling and mathematical analysis of swarms of microscopic robots", in "Swarm Intelligence Symposium, 2005. SIS 2005. Proceedings 2005 IEEE", pp. 201–208 (IEEE, 2005).

Gardiner, C., *Stochastic methods* (Springer-Verlag, Berlin–Heidelberg–New York–Tokyo, 1985).

Gillespie, D. T., "The chemical Langevin equation", J. Chem. Phys. **113**, 1, 297–306 (2000).

Grubb, G., *Distributions and operators*, vol. 252 (Springer, 2008).

Ha, S.-Y. and E. Tadmor, "From particle to kinetic and hydrodynamic descriptions of flocking", arXiv preprint arXiv:0806.2182 (2008).

Hamann, H. and H. Worn, "A space-and time-continuous model of self-organizing robot swarms for design support", in "Self-Adaptive and Self-Organizing Systems, 2007. SASO'07. First International Conference on", pp. 23–23 (IEEE, 2007).

Hundsdorfer, W. and J. G. Verwer, *Numerical solution of time-dependent advection-diffusion-reaction equations*, vol. 33 (Springer, 2003).

Kac, M., "Can one hear the shape of a drum?", American Mathematical Monthly pp. 1–23 (1966).

Kachroo, P., *Pedestrian dynamics: Mathematical theory and evacuation control* (CRC Press, 2009).

Khapalov, A. Y., *Controllability of partial differential equations governed by multiplicative controls* (Springer, 2010).

Kirsch, A., *An introduction to the mathematical theory of inverse problems*, vol. 120 (Springer, 2011).

Kurdila, A. J. and M. Zabarankin, *Convex functional analysis* (Springer, 2006).

Lenhart, S., "Optimal control of a convective-diffusive fluid problem", Mathematical Models and Methods in Applied Sciences **5**, 02, 225–237 (1995).

Leveque, R. J., *Finite-Volume Methods for Hyperbolic Problems* (Cambridge Univ. Press, 2004).

Lustig, M., D. Donoho and J. M. Pauly, "Sparse mri: The application of compressed sensing for rapid mr imaging", Magnetic resonance in medicine **58**, 6, 1182–1195 (2007).

Ma, K. Y., P. Chirarattananon, S. B. Fuller and R. J. Wood, "Controlled flight of a biologically inspired, insect-scale robot", Science **340**, 6132, 603–607 (2013).

Matthey, L., S. Berman and V. Kumar, "Stochastic strategies for a swarm robotic assembly system", in "Robotics and Automation, 2009. ICRA'09. IEEE International Conference on", pp. 1953–1958 (IEEE, 2009).

Milutinovic, D. and P. Lima, "Modeling and optimal centralized control of a large-size robotic population", Robotics, IEEE Transactions on **22**, 6, 1280–1285 (2006).

Murray, J. D., "Mathematical biology i: An introduction, vol. 17 of interdisciplinary applied mathematics", (2002).

Okubo, A., "Dynamical aspects of animal grouping: swarms, schools, flocks, and herds", Advances in biophysics **22**, 1–94 (1986).

Palmer, A. and D. Milutinovic, "A hamiltonian approach using partial differential equations for open-loop stochastic optimal control", in "American Control Conference (ACC), 2011", pp. 2056–2061 (IEEE, 2011).

Pinnau, R. and M. Ulbrich, *Optimization with PDE constraints*, vol. 23 (Springer, 2008).

Prorok, A., N. Corell and A. Martinoli, "Multi-level spatial modeling for stochastic distributed robotic systems", The International Journal of Robotics Research p. 0278364911399521 (2011).

Roos, H.-G., M. Stynes and L. Tobiska, "Robust numerical methods for singularly perturbed differential equations", Springer Ser. Comput. Math **24** (2008).

Sánchez-Garduño, F. and V. F. Breña-Medina, "Searching for spatial patterns in a pollinator–plant–herbivore mathematical model", Bulletin of mathematical biology **73**, 5, 1118–1153 (2011).

Simon, J., "Compact sets in the spacel p (o, t; b)", Annali di Matematica pura ed applicata **146**, 1, 65–96 (1986).

Stevens, A. and H. G. Othmer, "Aggregation, blowup, and collapse: the abc's of taxis in reinforced random walks", SIAM Journal on Applied Mathematics **57**, 4, 1044–1081 (1997).

Tagiev, R., "Optimal coefficient control in parabolic systems", Differential Equations **45**, 10, 1526–1535 (2009).

Tröltzsch, F., *Optimal control of partial differential equations: theory, methods, and applications*, vol. 112 (American Mathematical Soc., 2010).

Turpin, M., N. Michael and V. Kumar, "Capt: Concurrent assignment and planning of trajectories for multiple robots", The International Journal of Robotics Research **33**, 1, 98–112 (2014).

Vries, D., K. Keesman and H. Zwart, "A Luenberger observer for an infinite dimensional bilinear system: a UV disinfection example", (International Federation of Automatic Control, 2008).